EFFECTS OF FELDSPAR ADDITION ON PHASE FORMATION OF $CaCu_3Ti_4O_{12}$

by

AMIR SYAIFUDDIN BIN JUHARI

A thesis submitted in fulfillment of the requirements for the degree of Bachelor of Applied Science (Materials Technology) with Honours

FACULTY OF EARTH SCIENCE
UNIVERSITI MALAYSIA KELANTAN

2017

DECLARATION

I declare that this thesis entitled "EFFECTS OF FELDSPAR ADDITION ON PHASE FORMATION OF $CaCu_3Ti_4O_{12}$" is the result of my own research except as cited in the references. The thesis has not been accepted for any degree and is not concurrently submitted in candidature of any other degree.

Student:

Name: AMIR SYAIFUDDIN BIN JUHARI

Date:

ACKNOWLEDGEMENT

First of all, I would like to take this great opportunity to express my sincere gratitude and thank you to my supervisor, Dr. Muhammad Azwadi Bin Sulaiman and my co-supervisor, Dr. Muhamad Najmi Bin Masri for their invaluable sharing of knowledge, comments, ideas and advices about this final year projects. There were very patient and concern about the problems that I have during the experimental progress and they also help to find the best solutions to overcome the problems to make sure that the project was succeed. Besides, they also love to share their previous experience during conduct the experiment to make sure that I do not repeat the same mistakes.

Secondly, I would like to thank to my parents, Nor 'Aini Binti Mohd Idris that always giving me moral supports and always understand my situation during my final year progress. They also always giving me advices to focusing and did efficient work since Final year project I. There advices made me work harder and never give up during experimental failure occurred.

Then, I also want to give a thousand thank to all my friends in UMK Jeli Campus that also help me and giving me continuous supports during this project. They were very kind to teach me how to use a few machines and software to make me work faster without making any mistakes.

Finally, I would like to separate my sincerest gratitude to my friends' advisor Nurul Zaffiqa Binti Zamzuri, Nur Afiqah Binti Bakri, Siti Zuraina Binti Nawawi, Wan Marinah Izzati Binti Wan Ismail and all my course lecturers and laboratory assistant whom were always willing to help advices and share their knowledge to me directly and indirectly to finish up this writing and experiment successfully.

Effects of Feldspar Addition on Phase Formation of $CaCu_3Ti_4O_{12}$

ABSTRACT

The electroceramic of calcium copper titanate ($CaCu_3Ti_4O_{12}$, CCTO) was prepared by solid state reaction method by using three raw materials of calcium carbonate ($CaCO_3$), copper oxide (CuO) and titanium oxide (TiO_2) powders. This study was focused in characterization of pure and feldspar added CCTO properties such as surface microstructure and dielectric properties. The raw materials were weighted according to stoichiometric ratios to form pure CCTO. For feldspar addition CCTO, felspar was added with weight percentage ratio of 1%, 3%, 5%, 7% and 10%. The mixed powders were ball mixed for 24 hours using dry mixing. The mixed powder was calcined at 900°C with soaking time for 12 hours by using high temperature furnace. Then, the calcined powder was pressed into pellet form with 6 mm of diameter. The green pallet was sintered in furnace at 1040°C for 10 hours. Phase structure and surface microstructure were analyzed by using X-ray Diffraction (XRD) and optical microscope (OM). The single phase of CCTO was obtained after sintering process. The grains size become smaller for the increasing weight percentage of feldspar in CCTO hence the porosity of the CCTO samples decreases. Based on dielectric results, the 10 wt% of feldspar addtion CCTO gave the better dielectric properties.

Kesan Penambahan Feldspar ke atas Pembentukan Fasa bagi $CaCu_3Ti_4O_{12}$

ABSTRAK

Bahan elektroseramik kalsium kupro titanat ($CaCu_3Ti_4O_{12}$, CCTO) telah disediakan dengan kaedah tindak balas pepejal menggunakan tiga jenis bahan mentah iaitu kalsium karbonat ($CaCO_3$), titanium dioksida (TiO_2) dan kuprum oksida (CuO). Kajian ini merangkumi beberapa aspek pencirian bagi sifat-sifat CCTO tulen dan CCTO yang ditambah dengan feldspar seperti mikrostruktur permukaan dan dielektrik. Bahan mentah telah ditimbang mengikut nisbah stoikiometri untuk menghasilkan CCTO tulen. Bagi penyediaan CCTO yang ditambah dengan feldspar, bahan feldspar telah ditambahkan ke dalam campuran stoikiometri CCTO tulen dengan peratusan berat 1%, 3%, 5%, 7% dan 10%. Proses pencampuran dilakukan dengan menggunakan kaedah pencampuran bebola selama 24 jam dengan kaedah pencampuran kering. Campuran serbuk telah dikalsin pada suhu 900°C selama 12 jam menggunakan relau. Serbuk yang telah dikalsin dibentuk menjadi pelet bergaris diameter pusat 6 milimeter. Untuk kaedah lazim, pelet disinter pada suhu 1040°C selama 10 jam didalam relau. Fasa struktur dan mikrostruktur permukaan telah dianalisis menggunakan XRD dan mikroskop optik. Fasa tunggal telah diperoleh pada sampel yang telah disinter. Saiz butiran didapati semakin mengecil dengan penambahan peratusan berat bahan feldspar sekaligus mengurangkan keliangan sampel. Berdasarkan keputusan ujian dielektrik, sampel yang mempunyai 10% feldspar dalam CCTO memberi sifat-sifat pemalar elektrik yang lebih baik.

TABLE OF CONTENTS

LIST OF TABLES

LIST OF FIGURES

LIST OF ABBREVIATIONS

CCTO	Calcium Copper Titanium Oxide
CuO	Copper Oxide
TiO_2	Titanium Oxide
$CaCO_3$	Calcium Carbonate
XRD	X-Ray Diffraction
TG/DTA	Thermogravimetric/Differential Thermal Analysis
OM	Optical Microscope
TGA	Thermogravimetric Analysis
g/mol	gram per mol

LIST OF SYMBOLS

θ	Theta
°C	Degree Celcius
Mpa	Mega Pascal
K	Temperature
°	Degree
h	Hours
mm	millimeter
m	meter
Hz	Hertz
GHz	Giga Hertz
MHz	Mega Hertz
F	Speed
%	percentage
g	gram
mol	mol
cm	centimeter

CHAPTER 1

INTRODUCTION

1.1 Background of study

Advancement in technology leads scientist create many finding to enhance the performance and properties of advance materials. Ceramics is well known materials that have unique properties such as magnetic, optical and electrical properties. Combination of unique properties of advance ceramics can be exploited in a host of new products. Electroceramics is one of the example of advance materials. Electroceramics can be tailored to operate as ferroelectric materials, insulators, highly conductive ceramics, electrodes as well as sensors and actuators.

A dielectric material is one that is electrically insulating (nonmetallic) and exhibit or may be made to exhibit an electric dipole structure. The ability of dielectric materials to store charge, good insulator and poor conductor of electric current suitable for capacitor application.

Calcium Copper Titanium Oxide (CCTO) got attention from many researcher because the dielectric constant is stable from 100 – 600K (Bender & Pan, 2005) and has very small temperature dependence in a wide temperature range from 100 to 400K (Sulaiman *et al*., 2011) make it most suitable for capacitors, resonators and filter. There are different modes of CCTO synthesis process such as solid state reaction, sol gel method and precursor route.

1.2 Problem Statement

CCTO have high dielectric constant that important in miniaturization of electronic devices. However, high dielectric loss of CCTO restricts its further application. On of the solution to overcome this problem is mixed CCTO with another materials. Feldspar is the suitable materials that can enter into the air gap of CCTO and reduce the dielectric loss during sintering process.

1.3 Objectives

The objectives of this research are: -

1.3.1 To synthesize and characterize pure CCTO and feldspar added CCTO.

1.3.2 To reduce dielectric loss of CCTO by addition of feldspar.

1.4 Expected Outcome

A low loss dielectric material based on CCTO can be used to produce many electronic devices such as resonator antenna, resistor, capacitor and actuator. High performance and smaller size of devices is desirable with high effectively and this can be done by using advance materials such as CCTO.

CHAPTER 2

LITERATURE REVIEW

2.1 Introduction

The study of CCTO ceramics was discovered by scientist in several years lately. Dielectric properties on these ceramics make it suitable for capacitor application. However, the dielectric loss of CCTO ceramics is also high. In this study, addition of feldspar in CCTO ceramics was highlighted in order to reduce and overcome the dielectric loss in this material.

2.2 Electroceramics

In this new era, many of modern technologies use advance ceramics because of their unique electrical, mechanical, chemical, optical and magnetic properties and combination of these properties (Callister & Rethwisch, 2007). Electroceramics gain attention for potential application in miniaturized electronic devices or component (Li *et al*., 2009) such as telecommunication (Brizé et al., 2009) and aerospace (Marinescu, 2007). Other electroceramics that commonly used are lead zirconate titanate (PZT) (Chen *et al*., 2008), barium titanate ($BaTiO_3$) (Felgner *et al*., 2004), lead titanate ($PbTiO_3$) (Ye, 2013), zinc oxide (Wang, 2004) and CCTO. CCTO likes other electroceramics have extraordinary dielectric properties. The dielectric constant of CCTO is 10000 at room temperature (Sulaiman *et al*., 2013). It has independence temperature over range 100 – 400K (Amaral *et al*., 2011). Perovskite structure is important to develop new materials with high dielectric constant (Smith *et al*., 2009).

A dielectric material is materials that have electrical insulator (nonmetallic) and exhibits or may be made to exhibit an electric dipole structure that separate

negative and positive charged entities on molecular or atomic level (Callister & Rethwisch, 2007).

2.3 Processing of CCTO

The most commonly technique to process CCTO ceramics are solid-state reaction. This process consists of chemical decomposition reaction which is heating the solid reactant to produce a new solid plus gas. This reaction is commonly used to produce powders of simple oxide such as carbonates, nitrates, hydroxides, acetates, sulfates, alkoxides, oxalates, and other metal salts. This process involves mixing, calcination, shaping and sintering.

2.3.1 Raw Materials

Basic raw materials of CCTO are powder of calcium carbonate ($CaCO_3$), copper oxide (CuO) and Titanium Oxide (TiO_2) (Juliewatty *et al*., 2009). $CaCO_3$ is one of the most widely studied systems on decomposition. Decomposition of CCTO can be defined in Equation 2.1:

$$\mathbf{CaCO_3\,(\textit{s})} \rightarrow \mathbf{CaO\,(\textit{s})} + \mathbf{CO_2\,(\textit{g})} \ldots\ldots \textbf{(Equation 2.1)}$$

The standard heat (enthalpy) of reaction of $CaCO_3$ at 298K reported by Rahaman, 2006. Copper Oxide (CuO) ceramics is simple compound can easily prepared in pure form and available in large scale (Putjuso *et al*., 2011). Titanium Oxide (TiO_2) or titanate ceramics such as barium titanate ($BaTiO_3$) made to have extremely high dielectric constants which useful for capacitor application (Callister & Rethwisch, 2007). Feldspar is the most common mineral on the earth that making up more than half of the earth's crust. The term of feldspar can define as any of a group of natural crystalline aluminum silicate minerals containing sodium, potassium, calcium or

barium (Obstler *et al*., 2012). The general characteristics of feldspar are the formation of glassy, white surface when it was fired in stoneware temperature. Feldspar also has very long range of melting action from 1170°C to 1305°C. Melted feldspar possess a high surface tension because of their considerable alumina content (17% – 25%), they crawl and flow unevenly (Obstler *et al*., 2012)

2.3.2 Mixing

Mixing of $CaCO_3$, CuO & TiO_2 powder is important in order to make these materials become uniform and homogenized. Milling is the tools to mix the powder. Other purpose of milling also reduces particle size of powder. Milling consists of wet-ball milling and dry-ball milling. Wet-ball milling usually used water since it is available with adequate purity at low cost, non-flammable and non-toxic. The disadvantages of wet-ball milling is liquid must be removed by several way like evaporation by using oven. However, for electronic application, the usage of solvent such as ethanol and acetone is more preferred and need evaporation process.

The suitable time of milling process is important. Almeida *et al*., 2002 reported that increasing of milling time leads to the formation of nanocrystalline CCTO. Hutagalung *et al*., 2009 also state that milling process needs a very long time up to 100 h to obtain single phase of CCTO. The lack of time consuming during milling process affected non-homogeneous mixed of sample. Zirconia & alumina ball are widely used as milling media (Ni & Chen, 2009).

2.3.3 Calcination

Calcination is one of the heat treatment processes. This process causes constituents to interact by inter diffusion of their ions. Extend of diffusion was reduced during sintering process in order to obtain a homogeneous body (Moulson &

Herbert, 2003). Shorter calcination time and lower calcination temperature offered by modified mechanical alloying technique compared with conventional solid state reaction (Hutagalung et al., 2009). Calcination with high temperature and long duration is needed to obtain single phase CCTO body from a powder *(Hutagalung et al*., 2008). Reaction occurs in calcination process can be summarized in Equation 2.2:

$$CaCO_3(s)+3CuO(s)+4TiO_2(s)\rightarrow CaCu_3Ti_4O_{12}(s)+CO_2(g)$$ **..... (Equation 2.2)**

2.3.4 Pressing

Powder pressing is done after calcination process where powder is compacted into geometric form to make it solid or in pallet. There are several type of pressing which are uniaxial pressing and isostatic pressing that commonly used for compaction of dry powder (Rahaman, 2006). Mei *et al*., 2008 use cool isostatic pressing with a pressure 150 MPa. There are several research used high than that pressure. Marques et al., 2007 used 210 MPa of pressure by using isotactic pressing. Jacob *et al*., 2009 used 250 MPa in cool isotactic press. Juliewatty et al., 2009 used 300 MPa pressure of powder to be made in cylindrical specimen.

2.3.5 Sintering

Sintering is important technique in ceramics production. During sintering, the powder is heated to produce desire microstructure. The powder is heated under materials melting temperature. The powder does not melt, but the particle joint together and reduce porosity. Brizé *et al*., 2006 reported that dielectric properties are very sensitive to processing such as mixing, calcination, shaping and sintering. Scientists were looking for sintering process because of importance to find the right

sintering parameter such as temperature and duration (Juliewatty *et al*., 2009). Proper parameter of sintering process is important to ensure that small grain formation (2-5µm) with high dielectric constant will be obtained (Brizé *et al*., 2006; Prakash & Varma, 2007). Huang *et al.*, 2015 used two different temperatures as sintering parameters which are 1100°C for 3, 6 and 9 hours soaking time and second temperature at 1150°C then decreased to 1000°C immediately for 2, 3, 6, 8 hours soaking time. Juliewatty et al., 2009 used lower temperature which is 1040°C for 10 hours. Shri *et al*., 2008 sintered the CCTO pallet at 1025, 1050, 1075 and 1100°C for 10 hours.

2.4 Characterization

CCTO can be characterized by using X-ray Diffraction (XRD), Thermogravimetric/Differential Thermal Analysis (TG/DTA), Optical Microscope (OM), Density and Porosity Measurement and Dielectric Constant.

2.4.1 X-Ray Diffraction

X-Ray Diffraction (XRD) is method to study crystal structure and lattice spacing of materials. It also gives information on unit cell dimension. XRD is working based on Bragg's Law. Besides, XRD also give information about presence of element or compound in powder mixture. Sakamaki et al., 2010 obtained XRD pattern of phase composition of synthesized powder by using Rigaku D/MAX-2500 at 40kV and 100mA. Yun & Wang, 2006 report that CCTO is presence as single phase for Bi_2O_3 concentration up to 0.3. The peak pure CCTO of CuO could be seen and fade away after bismuth doping (Figure 2.1).

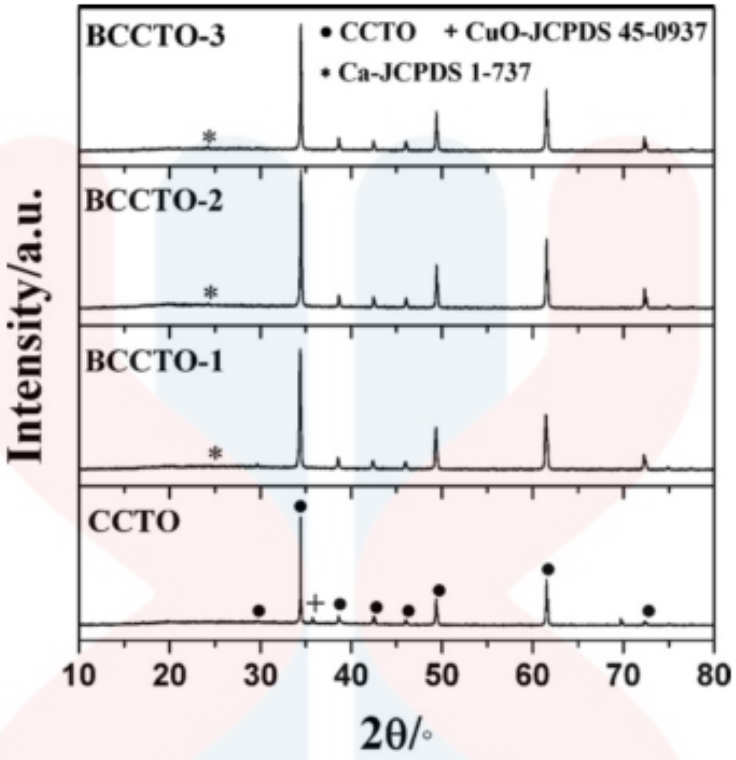

Figure 2.1: XRD pattern of the sintered CCTO ceramics (Yun & Wang, 2006)

Amaral *et al*., 2010 reported that CCTO is present in all sample as major phase. However, at lower calcination temperature (700°C) secondary phase like CuO and TiO_2 are found. Only residual signs of CuO can be detected at calcination above 800°C by XRD (Figure 2.2).

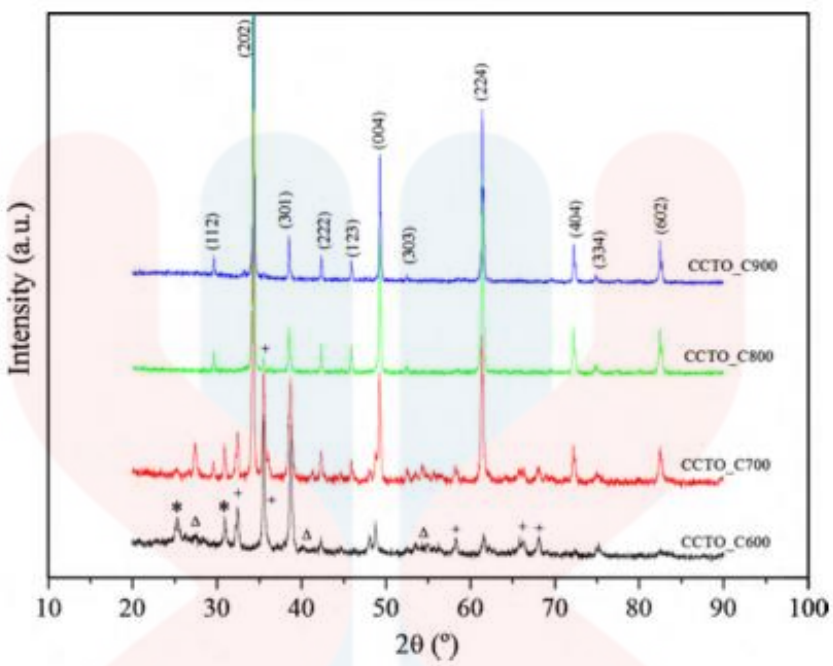

Figure 2.2: XRD Pattern for calcinated CCTO powder. There are indicated the index plane of the CCTO phase (Amaral *et al.*, 2010).

2.4.2 Thermogravimetric/Differential Thermal Analysis (TG/DTA)

TG/DTA commonly used to identify the burn off temperatures of ceramic containing such additives. Thomas *et al*., 2008 reported that strong exothermic peak observed around 478°C and an endotherm around 753°C for calcium oxalate (Figure 2.3). Zhu *et al*., 2009 reported that the result of TGA and DTA curves shows three stages of weight loss where the first one is in the temperature range in room temperature to 250°C, the second one is from 250 - 400°C and the third one is around 700°C (Figure 2.4). Rai *et al*., 2009 was reported that the result of TGA/DTA shows three stages of small weight loss in the temperature range up to 400°C. A sharp weight loss occurs in the temperature range 400 - 500°C. Very slight weight loss occurs up to 800°C. (Figure 2.5)

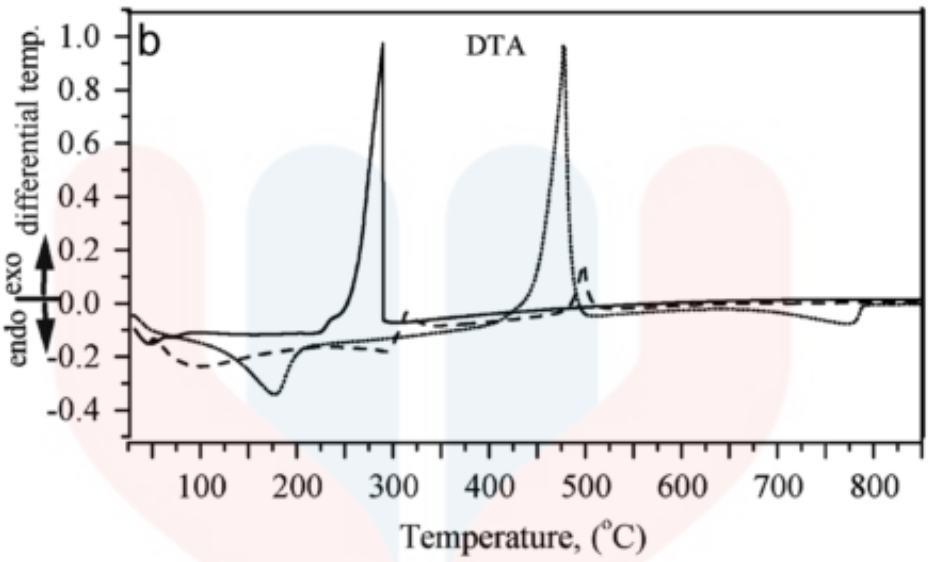

Figure 2.3: DTA of the individual oxalates, namely, calcium oxalate, titanyl oxalate and copper oxalate (Thomas *et al*., 2008)

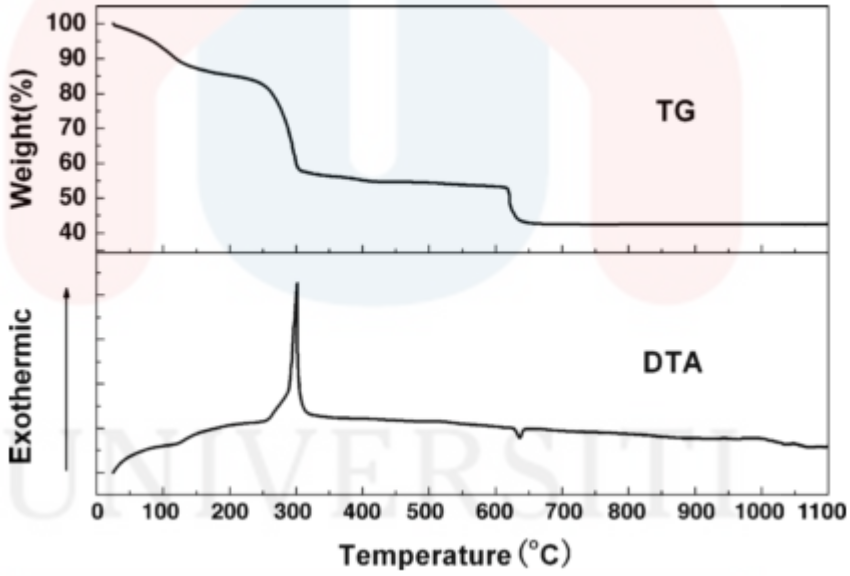

Figure 2.4: DTA-TGA curve of CCTO (Zhu *et al*., 2009)

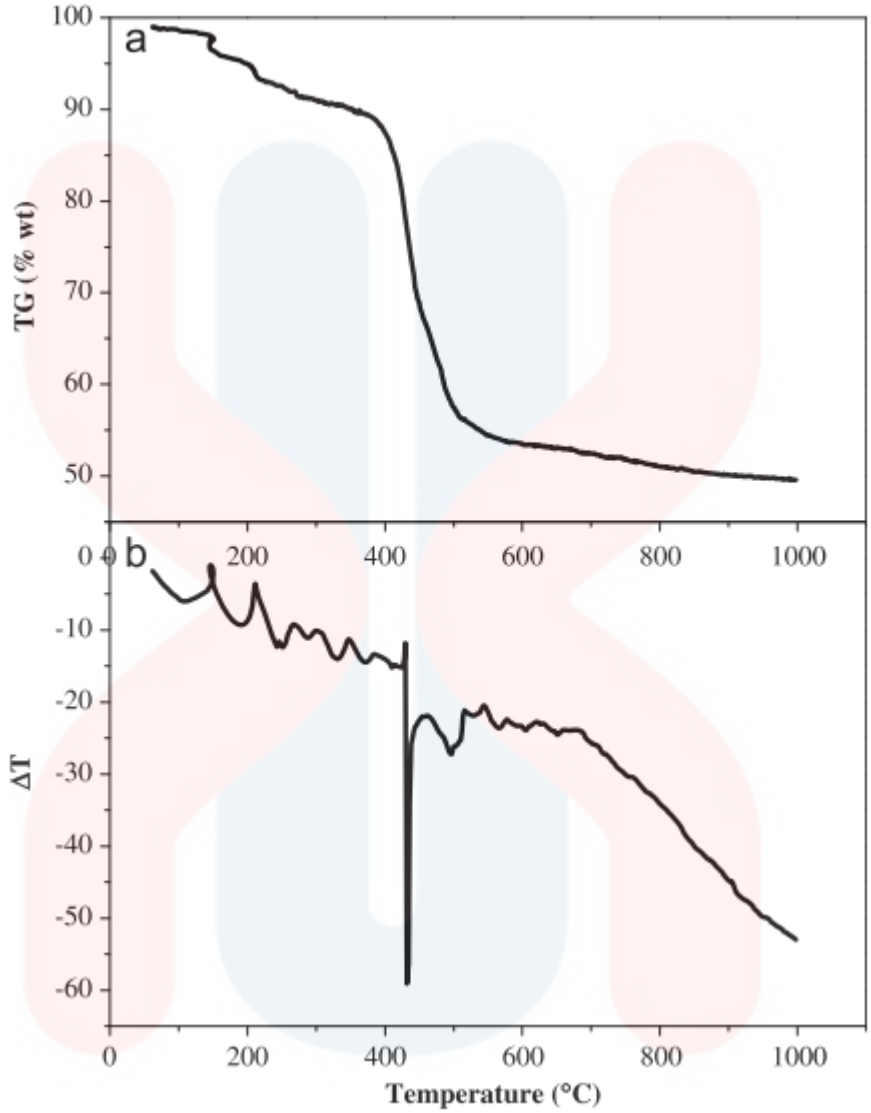

Figure 2.5: TGA/DTA plots of $Ca_{1-3x/2}La_xCu_3Ti_4O_{12}$ for (x = 0.30) (Rai *et al*., 2009)

2.4.3 Optical Microscope

Optical microscope is used to study surface morphology of sample (George & Sebastian, 2009). Besides, optical microscope also used to determine cracks length and parameter of samples. Figure 2.6 shows the cracks initiation where average of six indentations was made on sample surface.

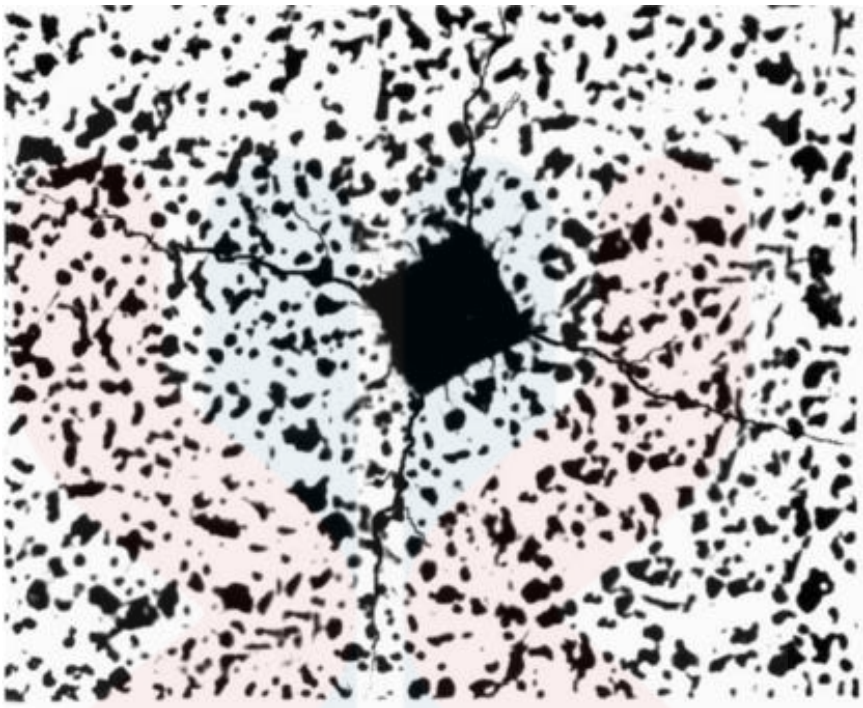

Figure 2.6: Optical micrograph revealing the crack originating from the corners of indentation (Panneerselvam *et al*., 2003)

2.4.4 Density & Porosity Measurement

Density of CCTO affected by sintering condition where increasing sintering temperature enhance density of sample (Mohamed *et al*., 2007). Besides, increasing of soaking time during sintering process also affected the density of CCTO. Table 2.1 shows density and shrinkage of sintered sample at different soaking time. Sun *et al*., 2007 reported that porosity decrease when densities with sintering time increase in 20-h sintered sample.

Table 2.1: Density and shrinkage of sintered samples (Huang et al., 2015)

Soaking time	2h	3h	6h	8h
Density(g/cm^3)	4.035	4.064	4.076	4.112
Shrinkage (%)	18.7	19.9	22.8	24.2

CHAPTER 3

MATERIALS AND METHOD

3.1 Introduction

Methodology is the main part of the research. This part describes the procedure and materials that used in synthesize and characterize CCTO ceramics formation using solid state reaction step by step. The research flow chart shown in Figure 3.1

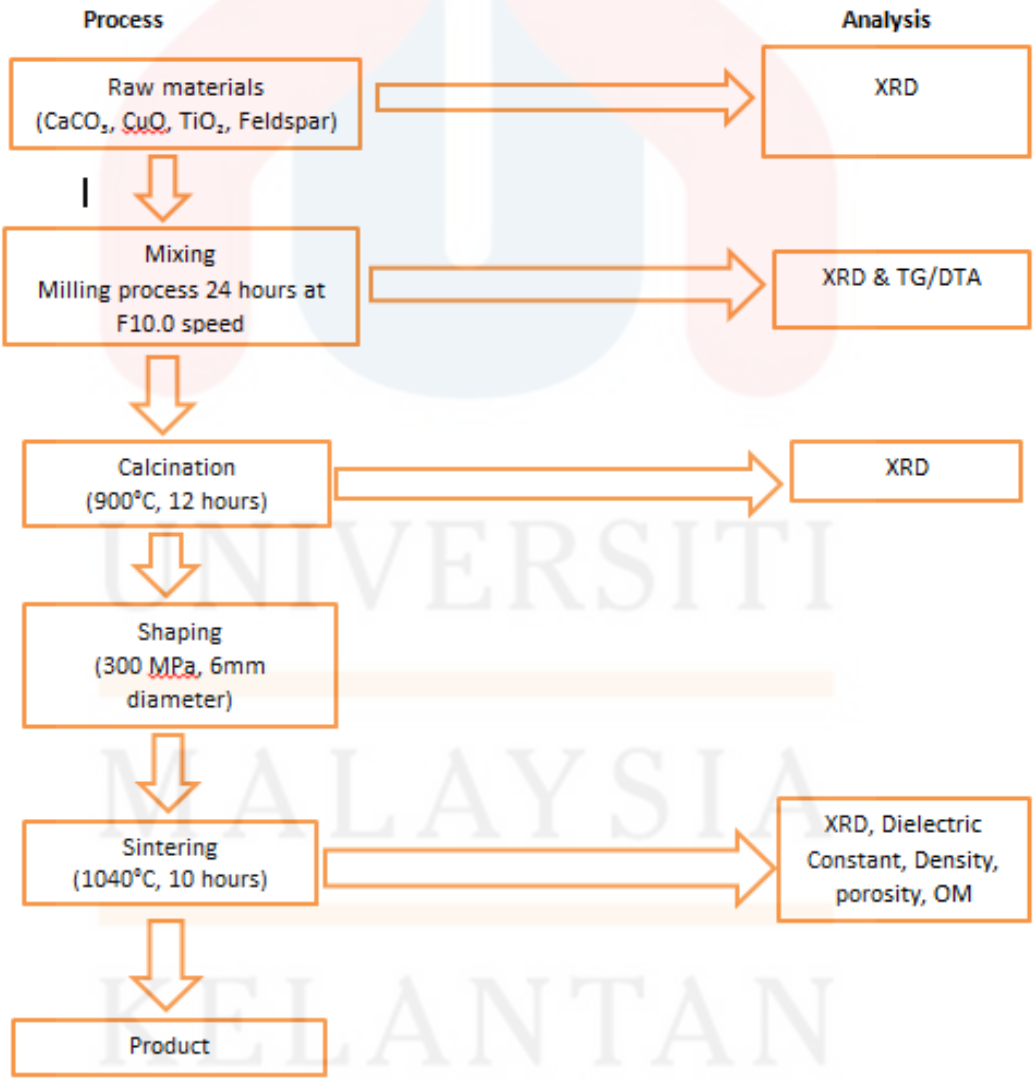

Figure 3.1: Research flow chart

3.2 Raw Materials

CCTO is combination from calcium carbonate ($CaCO_3$), copper oxide (CuO) and titanium oxide (TiO_2). For this study, feldspar also is added as raw materials. $CaCO_3$ that used in this study was supplied by Sigma-Aldrich, with >99% purity and the color of powder is white. CuO powder was supplied by Sigma-Aldrich with >99% purity and the color is black. TiO_2 powder was supplied by Merck with >99% purity and the color is white. Feldspar was supplied by Sibelco Malaysia and the color is white. All of raw materials are weight based on stoichiometry ratio and high precise balance up to four decimal places in order to get accurate reading. The mass of raw materials of CCTO is based on the Equation 2.2.

3.3 Mixing

The step of mixing is by using milling machine assisted by conventional alumina ball milling. The raw material is place in milling container with alumina ball milling and the ratio between raw materials and alumina ball milling is 1: 10. Milling process takes 24 hours at F10.0 speed constantly.

3.4 Calcination

After milling process, the sample is place at alumina crucible to undergo calcination process. The sample powder is calcined in furnace at 900°C for 12 hours.

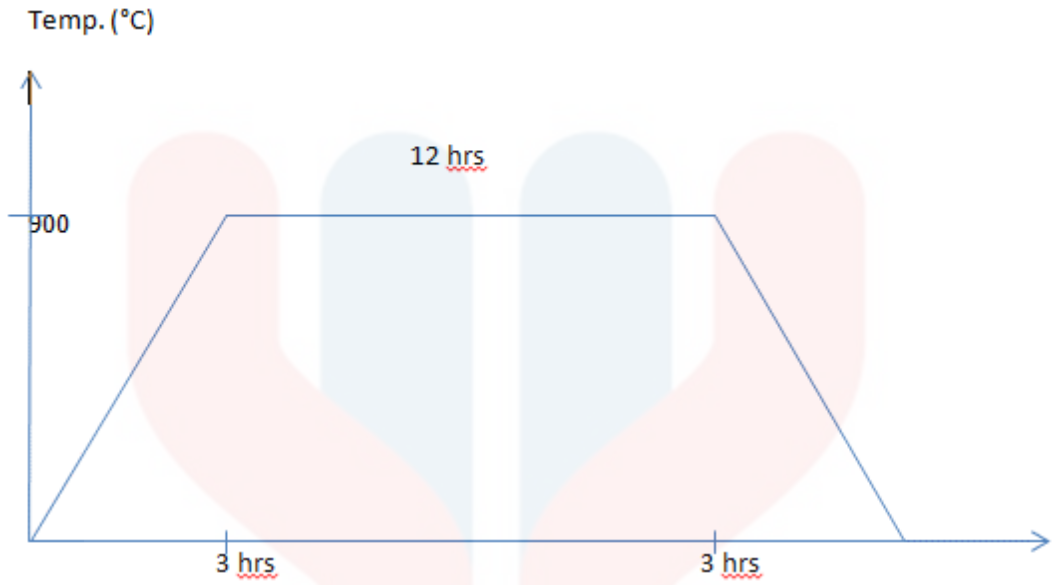

Figure 3.2: Heating profile for calcination process

3.5 Pressing

The sample powders are pressed into cylindrical with 6 mm diameter and 1 mm of thickness mold under 300 MPa until it become pellets. This process is conducted by using cool hand press machine.

3.6 Sintering

Pellet that produce from pressing process was sintered in air at 1040°C for 10 hours with heating rate 5°C per minute followed by cooling process in furnace temperature until reach room temperature. The pallet is place on modified feldspar crucible to avoid the crucible melt at higher temperature.

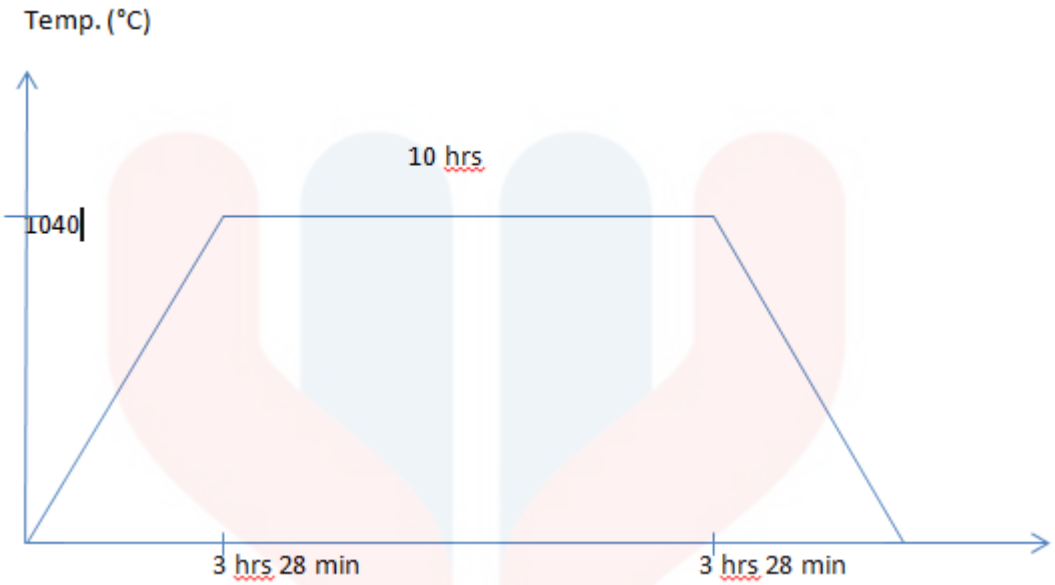

Figure 3.3: Heating profile for sintering process

3.7 Characterization

Characterization of CCTO is based on morphology, density, dielectric properties and mineralogy.

3.7.1 X-Ray Diffraction (XRD)

XRD is the non-destructive analysis technique used for analyzes crystal structure and phase identification of crystalline materials. XRD is working based on Bragg's Law. Bruker D2 Phaser XRD is one of the famous types of XRD and Diffract.Eva is example of software that gives specific information about the result of XRD analysis.

3.7.2 Density & Porosity Measurement

Archimedes's principle state that a body immersed in a fluid is buoyed up by a force equal to the weight of the displaced fluid. This principle is used in the density

measurement to measure bulk density of pallet. Bulk density referred to actual density of sample that consist big number of imperfection. It can calculate by using Equation 3.1:

$$\textbf{Bulk density} = \frac{MD}{MW-MS} \textbf{ x density of water ..... (Equation 3.1)}$$

Appearance porosity can be measured by using Equation 3.2:

$$\textbf{Appearance Porosity (\%)} = \frac{MV-MD}{MW-MS} \textbf{ x 100 ..... (Equation 3.2)}$$

Where,

M_D: mass of sample before vacuum

M_S: mass of sample in water

M_W: mass of sample after vacuum

3.7.3 Dielectric Measurement

Dielectric constant is measured by electroding the sample with silver paste using impedance analyser. The range is set from 1Hz – 10 GHz at 25°C of temperature. The formula to calculate dielectric constant as shown in Equation 3.3

$C = \in \frac{A}{l}$ **..... (1)**

$C = \in_r \in_\circ \frac{A}{l}$

$\in_r = \frac{Cl}{\in_\circ A}$

A : Cross area

l : Thickness

C : Capacitance

E_o : Universal Constant (8.85×10^{-12})

E_r : Dielectric Constant

3.7.4 Optical Microscope

Optical microscope is used to observe surface microstructure of material. It can reach at 5 x magnifications, 10 x magnifications and 15 x magnifications.

3.7.5 Thermogravimetric/Differential Thermal Analysis (TG/DTA)

TG/DTA was used to identify the burn off temperatures of ceramic containing such additives. TGA machine that was used is Mettler Toledo brand. The samples were weight before burns in TGA. The minimum temperature was set at 23°C and the maximum temperature was set at 900°C with heating rate 5°/min.

CHAPTER 4

RESULTS AND DISCUSSIONS

4.1 Introduction

This chapter discussed about results of effects of feldspar addition on phase formation of CCTO. The properties of raw materials are characterized first by using XRD before proceed to others process such as mixing, calcination, pressing and sintering by follow the sequence in Figure 3.1

4.2 Raw Material Characterization

Raw materials characterization is most important to final product and properties to ensure the CCTO is produce in high quality product. XRD is used to study initial properties of starting materials. Raw materials of CCTO were shows in Figure 4.1.

Figure 4.1: Raw materials of CCTO; (a) $CaCO_3$, (b) CuO, (c) TiO_2, (d) Feldspar

4.2.1 $CaCO_3$ Powder

$CaCO_3$ that used in this study was supplied by Sigma-Aldrich, with >99% and the colour of powder is white. $CaCO_3$ powder is shows in Figure 4.1(a). Figure 4.2 shows the x-ray diffraction (XRD) pattern of $CaCO_3$ powder to determine the phase that present. From the x-ray diffraction (XRD) pattern, the powder was confirmed as single phase of $CaCO_3$. $CaCO_3$ contains 83.4% of crystallinity and 16.6% of amorphous. The major peak at $2\theta = 29.2°$. The pattern number for $CaCO_3$ is COD 9015691.

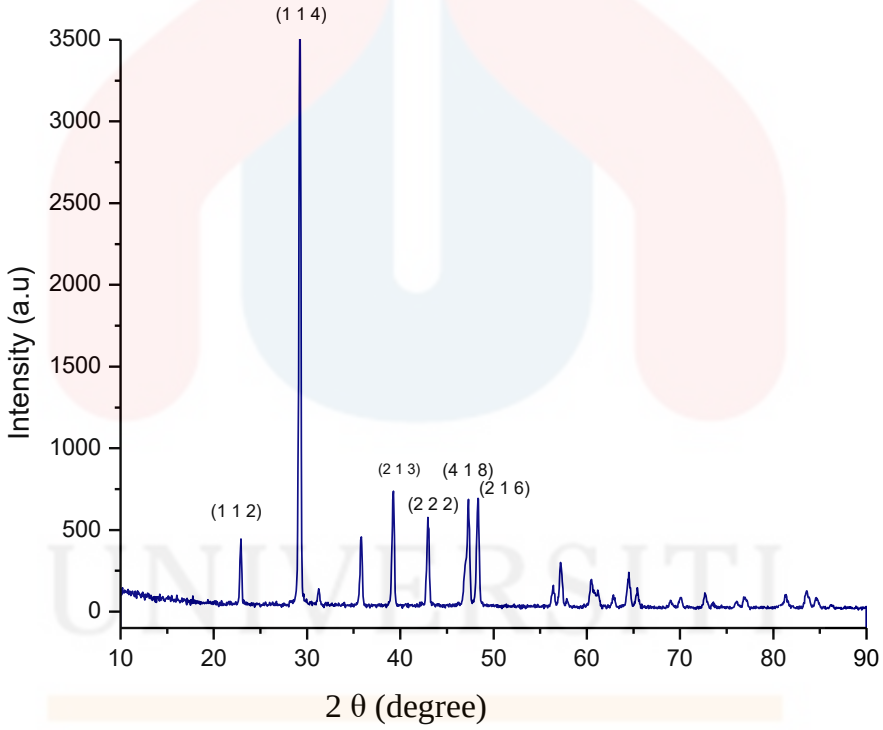

Figure 4.2: XRD Pattern of $CaCO_3$ (COD 9015691)

4.2.2 CuO Powder

CuO was supplied by Sigma-Aldrich with >99% purity and the powder is black in colour. CuO Powder is shows in Figure 4.1(b). X-ray diffraction pattern of CuO is show in Figure 4.3. The patterns have confirmed the existence of single phase

of CuO. CuO contains 82.4% crystallinity and 17.6% amorphous. The major peak at 2θ = 35.4°. The pattern number for CuO is COD 9015822.

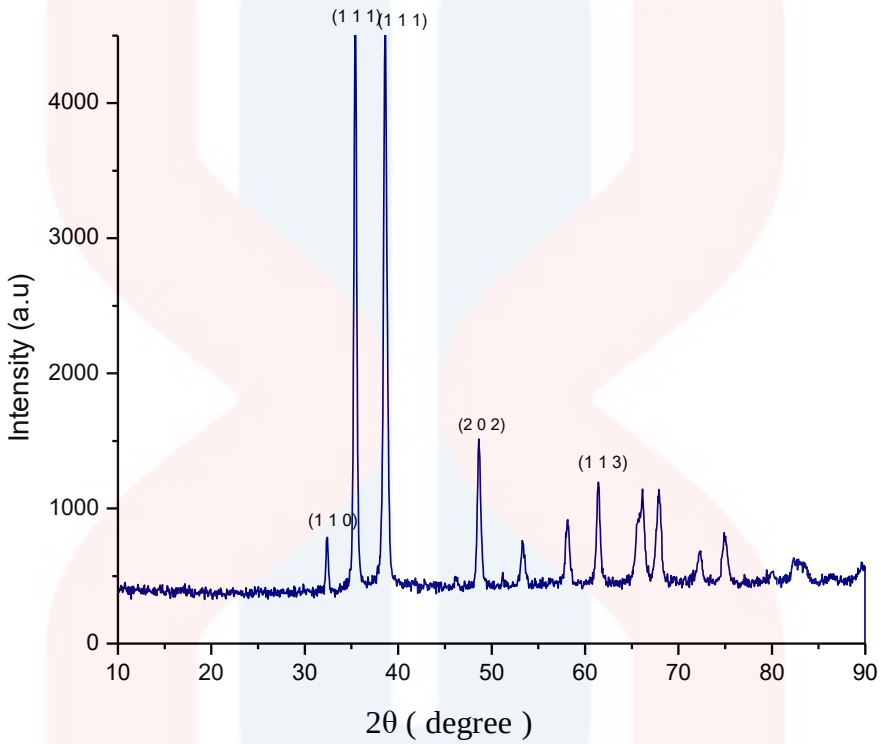

Figure 4.3: XRD Pattern of CuO (COD 9015822)

4.2.3 TiO_2 Powder

TiO_2 powder was supplied by Merck with >99% purity and the colour is white. TiO_2 powder is shows in Figure 4.1(c). Figure 4.4 shows the x-ray diffraction pattern of TiO_2 powder. The pattern was confirmed the existent of single phase of TiO_2. TiO_2 contains 78.3% of crystallinity and 21.7% of amorphous. The major peak at 2θ = 25.3°. The pattern number for TiO_2 is COD 7103589.

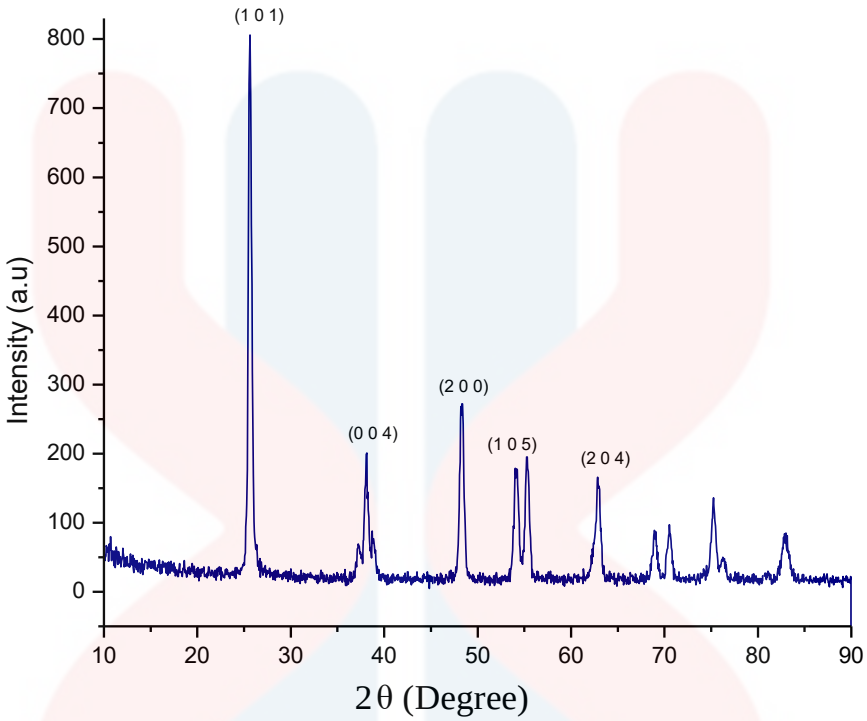

Figure 4.4: XRD Pattern of TiO_2 (COD 7103589)

4.2.4 Feldspar

Feldspar was supplied by Sibelco Malaysia in white colour. Feldspar is shows in Figure 4.1(d). Figure 4.5 shows x-ray diffraction of feldspar. Feldspar contains 79.3% of crystallinity and 20.7% of amorphous. The major peak at $2\theta = 27.6°$. The pattern number for feldspar is COD 9010841.

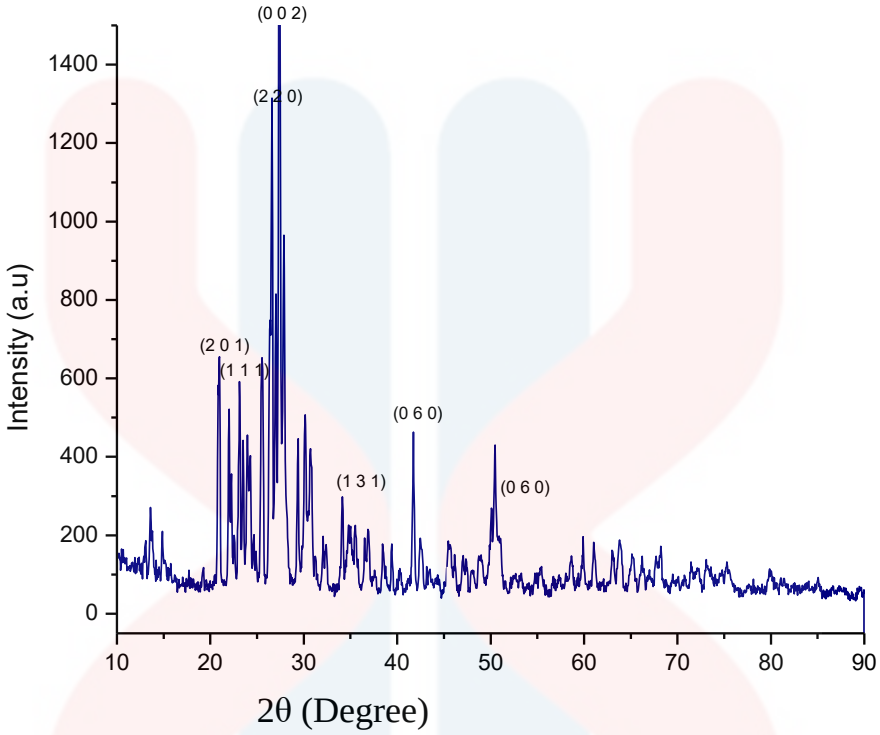

Figure 4.5: XRD Pattern of Feldspar (COD 9010841)

4.3 Mixing Process

CCTO samples were prepared by solid state method. The raw materials ($CaCO_3$, CuO, TiO_2 and feldspar) were weighted according stoichiometric ratio from CCTO. Feldspar has been used as addition material in this study. The materials is mixed and milled for 24 hours using mixing machine. Figure 4.6 shows the mixture powders resulted from mixing machine which is grey in colour.

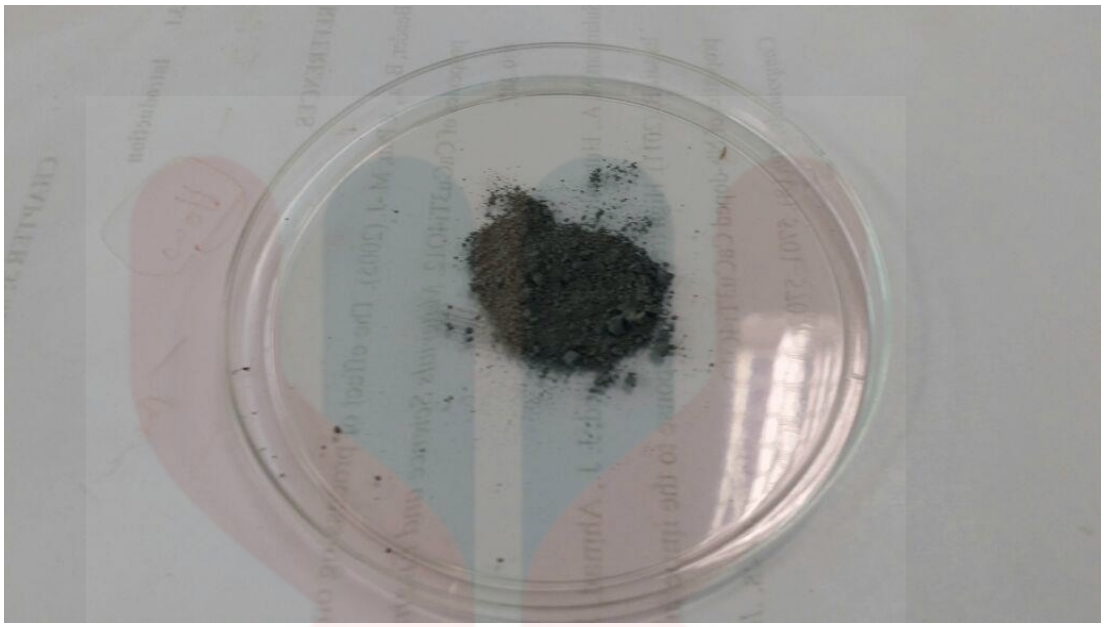

Figure 4.6: CCTO powder after mixing process for 24 hours

After the mixing process, the powder was analysed by X-ray diffraction (XRD). This analysis is to confirm the formation of CCTO after the mixing process. Figure 4.7 shows x-ray diffraction pattern of CCTO powder that mixed using different weight percentage of feldspar addition. The weight percentages of feldspar addition are 0, 1, 3, 5, 7 and 10 %. The presence of $CaCO_3$, CuO and TiO_2 was found in this stage. The major peak are (1 0 1), (1 1 4), (1 1 1), (2 0 0), (2 1 1) and (1 0 0).

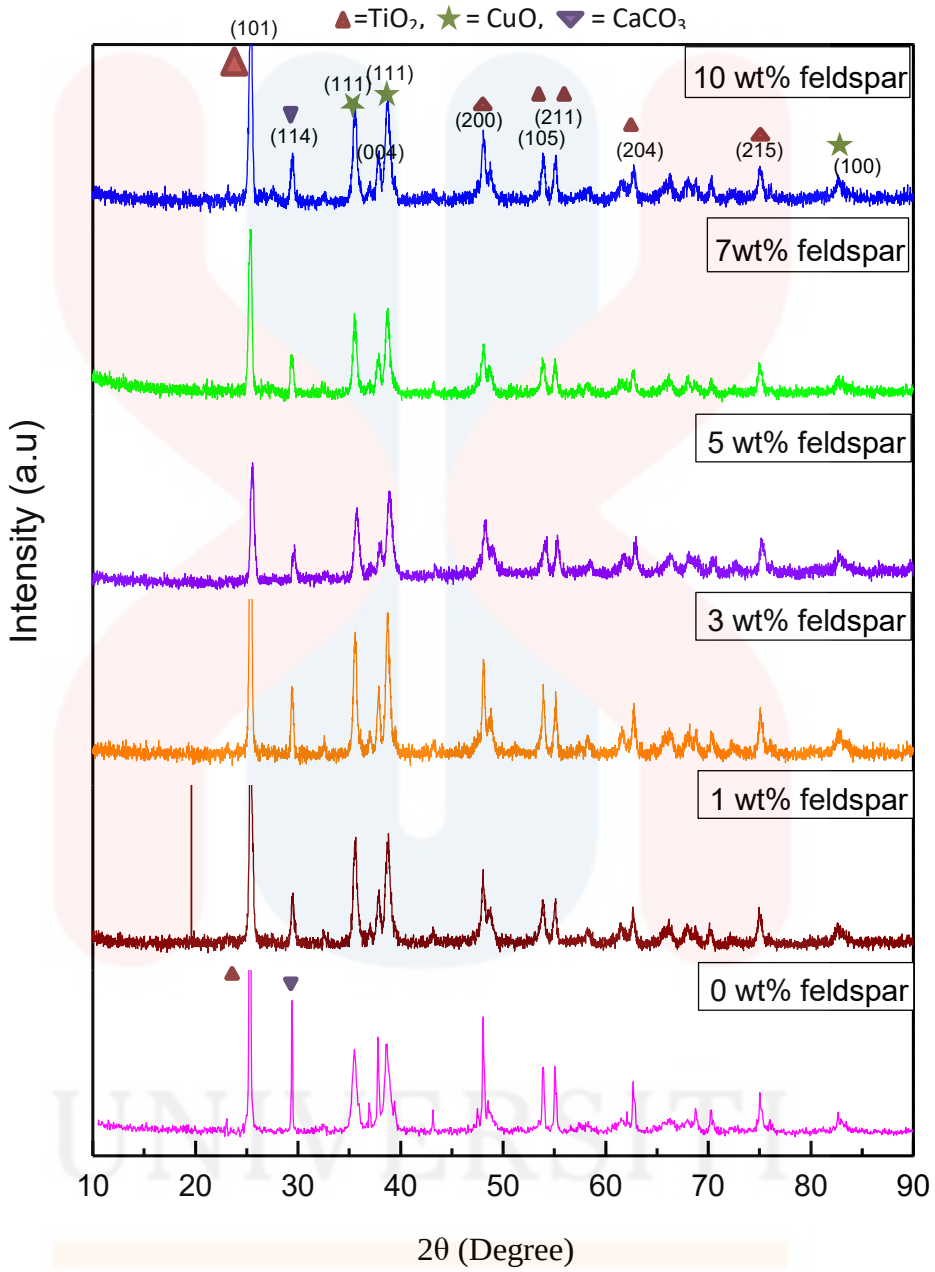

Figure 4.7: XRD Pattern of CCTO after mixing process

Before the mixing sample was calcined, the samples were test by using Thermogravimetric Analysis (TGA) to identify burn off temperature of CCTO ceramics. Figure 4.8 show result of thermogravimetric analysis (TGA) of mixed sample CCTO. There are two stages of weight loss of feldspar added samples where

the first one in range of temperature 150 - 250°C. The second stage of weight loss is in range of temperature from 350 to 425°C. 0wt% of feldspar sample also shows two stages of weight loss with different temperature than feldspar added samples. The first stage of weight loss of 0wt% of feldspar sample is in range of temperature from 125 to 250°C and the second stage from 350 to 425°C in range of temperature.

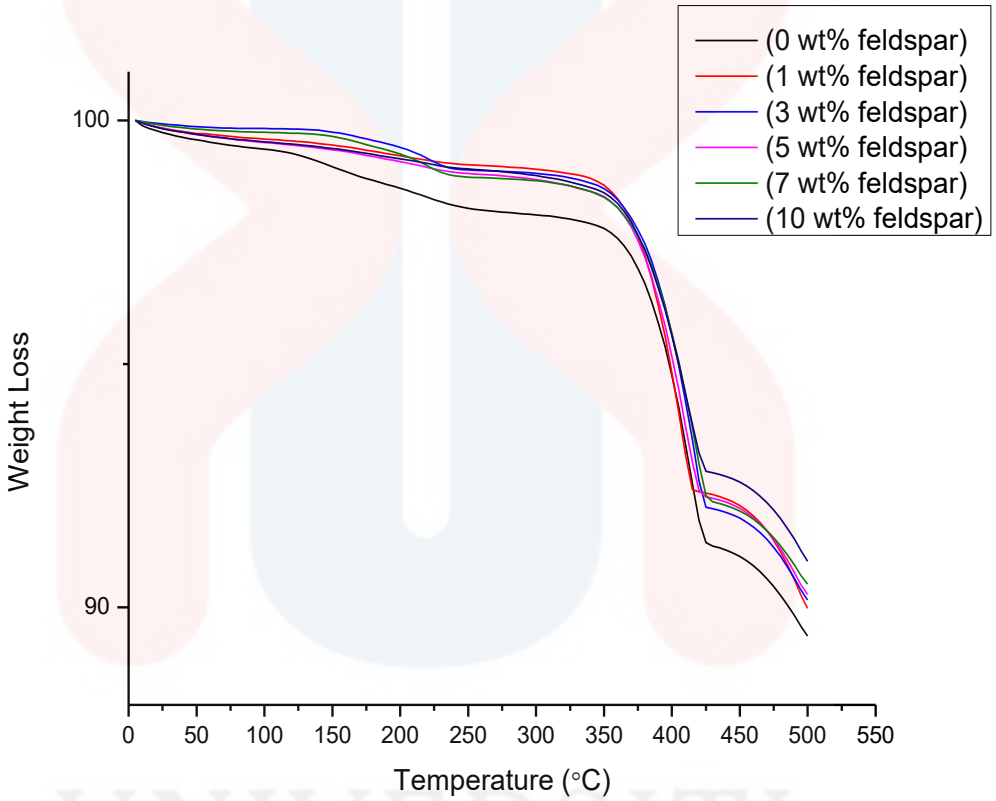

Figure 4.8: TGA result on mixing CCTO

4.4 Product Characterization

After mixing process, the samples undergo calcination process. Calcination process is applied the substance to the action of heat, but without fusion, for the purpose of causing some change in its physical or chemical constitution. The important factor of this process is to control the shrinkage during sintering. Figure 4.9 shows the calcined CCTO powder. The powder samples were calcined at temperature 900°C for 12 hours using furnace as shown in Figure 3.1. In this

process, the colour of mixed powder has been changes from grey (Figure 4.6) to yellowish after calcination process.

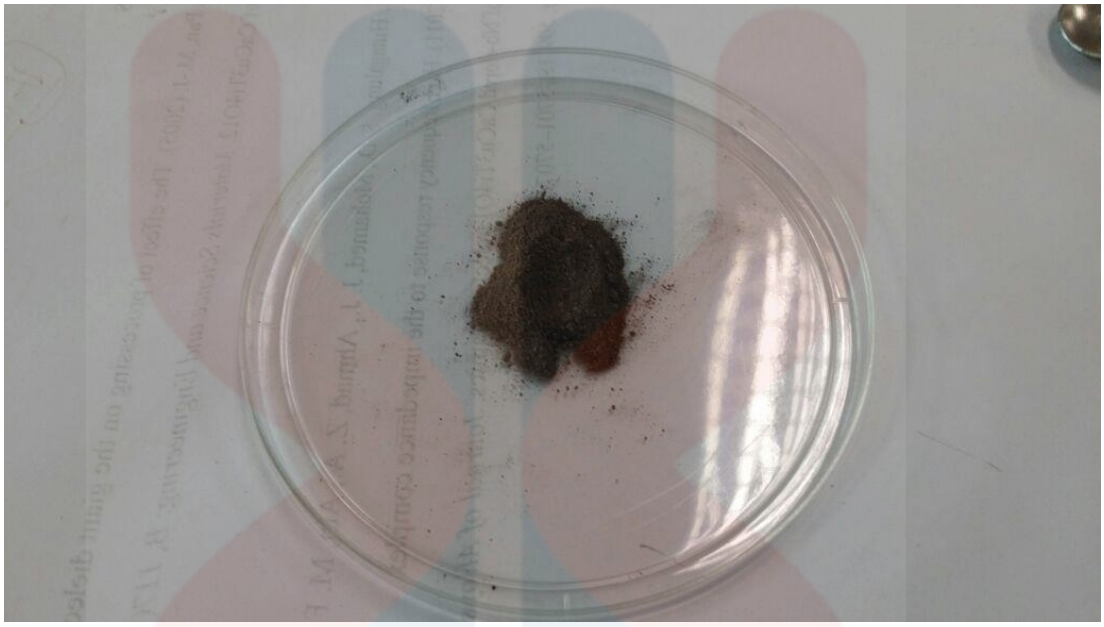

Figure 4.9: CCTO powder after calcination process at 900°C for 12 hours

The product after calcination was analysed by X-ray diffraction (XRD). The analysis of X-ray diffraction is to confirm the formation of CCTO after calcination process. Figure 4.10 shows the x-ray diffraction pattern of calcined CCTO using different weight percentage of feldspar addition. The weight percentages of feldspar addition in CCTO are 0, 1, 3, 5, 7 and 10 weight percentage.

Figure 4.10 shows the x-ray diffraction (XRD) analysis of calcined powder CCTO at 900°C for 12 hours. It was proved that the formation of single phase structure formation. There are no obvious differences between crystal phase of 0wt% of feldspar in CCTO sample and feldspar added CCTO samples. All the CCTO ceramics shows four major distinct (310), (440), (800) and (844). In Figure 4.10 also shows the presence of CuO and TiO_2 peaks which is not completely reacted to form CCTO. The presence of CuO and TiO_2 residue in calcined powder might be due to particle size incompletely milling process and calcination temperature.

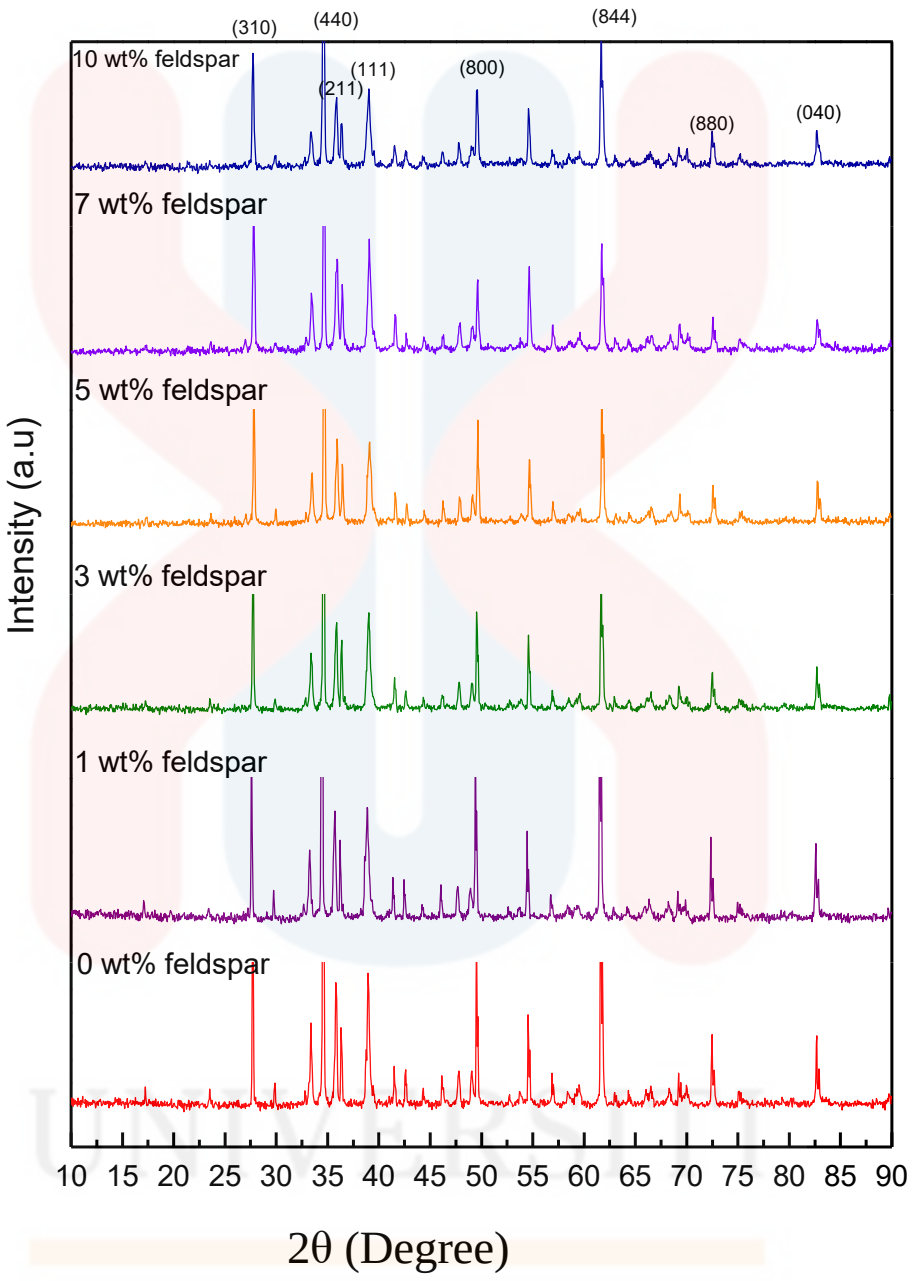

Figure 4.10: XRD Pattern of samples after calcination process

After calcination process, the calcined powder was compacted into a pellet with 6 mm in diameter. Before sintering process, the yellowish pellet is in green body. Sintering process is done to improve such compact properties as toughness,

electrical properties, strength, and densification. The pellet is in black colour after sintering process as shown in Figure 4.11.

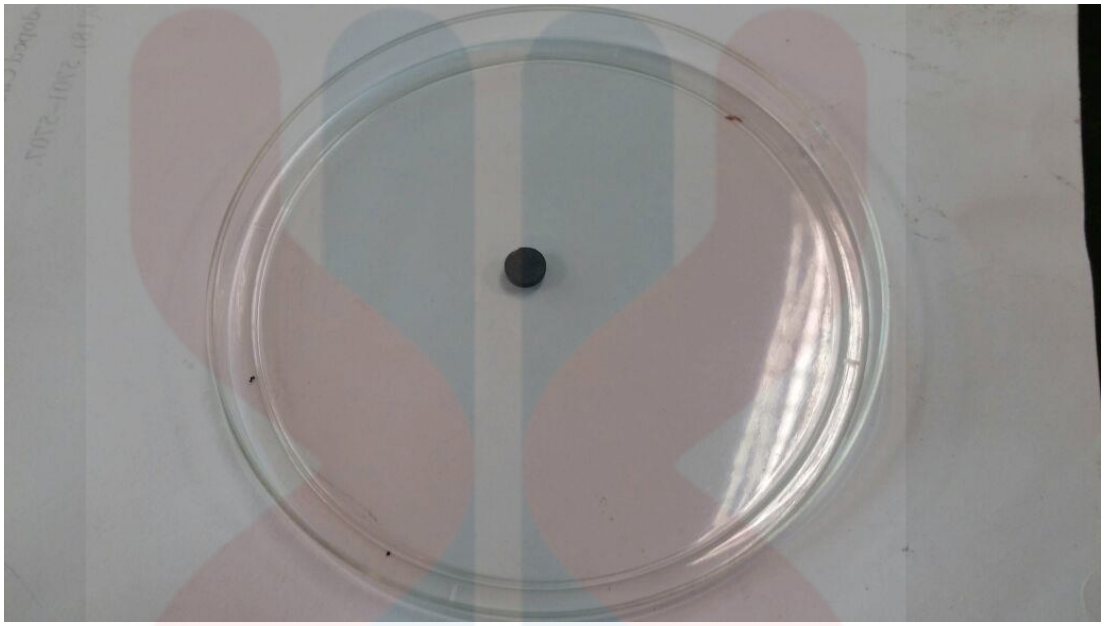

Figure 4.11: As-sintered CCTO at 1040°C for 10 hours

The pellets were sintered at 1040°C for 10 hours by using furnace with heating profile as shows in Figure 3.2. The powders were compacted into required shape to ensure the particle was contacted with each other in many sites. The structure of this green body has pore. The atom will diffuse to the particle boundary areas to reduce boundary energy and allows the particles to bond with each other and make the pore become shrinking at high sintering temperature. The samples become dense causes by elimination of pore if soaking time of sintering is carried long enough periods. The sample become black in colour and was analysed with x-ray diffraction (XRD).

Figure 4.12 shows the x-ray diffraction pattern of as-sintered CCTO at 1040°C for 12 hours. The pattern shows single phase of CCTO was obtained. The pattern shows five highest distinct; (220), (400), (422), (440) and (402). After sintering process, there are no TiO_2 peaks exist and it can be proved that the

formation of single phase structure of CCTO was completely formed. However, there are presences of CuO peak in 0wt% of feldspar addition sample and 1wt% of feldspar addition sample was detected by XRD.

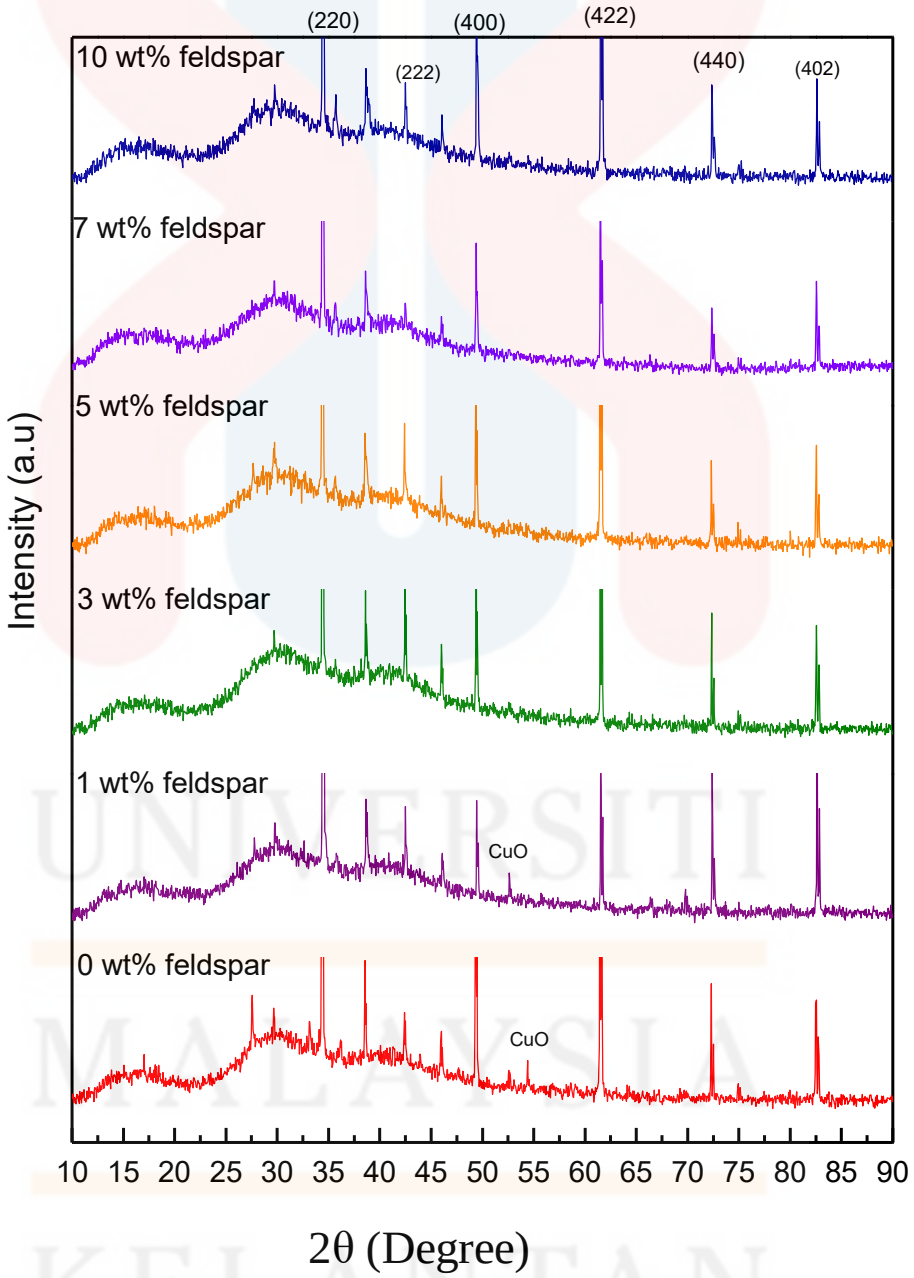

Figure 4.12: XRD Pattern of as-sintered CCTO at 1040°C for 10 hours with different weight percentage of feldspar addition

4.5 Surface Microstructure

Figure 4.13 shows the optical micrographs of as-sintered CCTO pellets at 1040°C for 10 hours with different weight percentage of feldspar addition using solid state method by using optical microscope (OM) with 5x magnification.

As observed, the microstructure of CCTO ceramics was change significantly with increasing addition of feldspar. From observation, the average grain size of as-sintered CCTO decreases as weight percentage of feldspar addition is increased. From this analysis, it was found that CCTO grains boundaries is covered by the light colored exfoliated sheet.

Figure 4.13 (a) shows the grain boundary of pure CCTO ceramics has rough surface and bigger than other samples. Figure 4.13 (c) shows the grains boundary has fine particles and become smaller. At Figure 4.13 (f) shows the finest microstructure of grain boundaries.

Feldspar particles were entering in the air gap of porous structure of CCTO and make the samples become dense after sintering process.

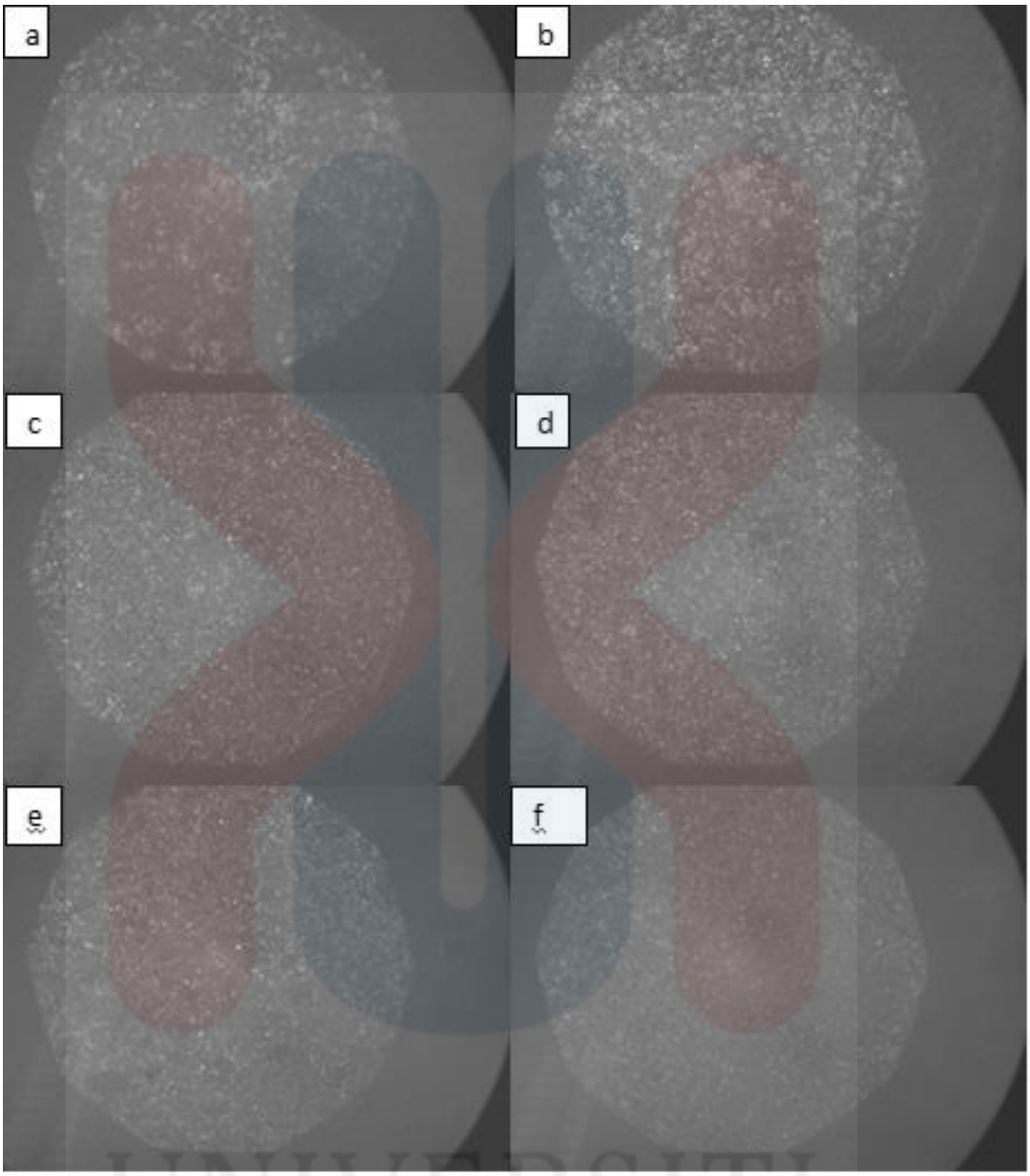

Figure 4.13: Microstructure of as-sintered CCTO with 5 x magnifications

4.6 Density and porosity

Archimedes method is used to measure density of as-sintered CCTO pellets. The result of the density measurement was shown in Figure 4.14. The density of as-sintered CCTO pellet is decrease drastically from pure as-sintered CCTO up to 1 wt. % of feldspar in CCTO. The bulk density is rose up from 1 wt. % of feldspar in CCTO to 3 wt. % of feldspar in CCTO before decrease again to 5 wt. % of feldspar

in CCTO. Then, it increase drastically to 7 wt. % of feldspar in CCTO and finally decrease to 10 wt. % of feldspar in CCTO.

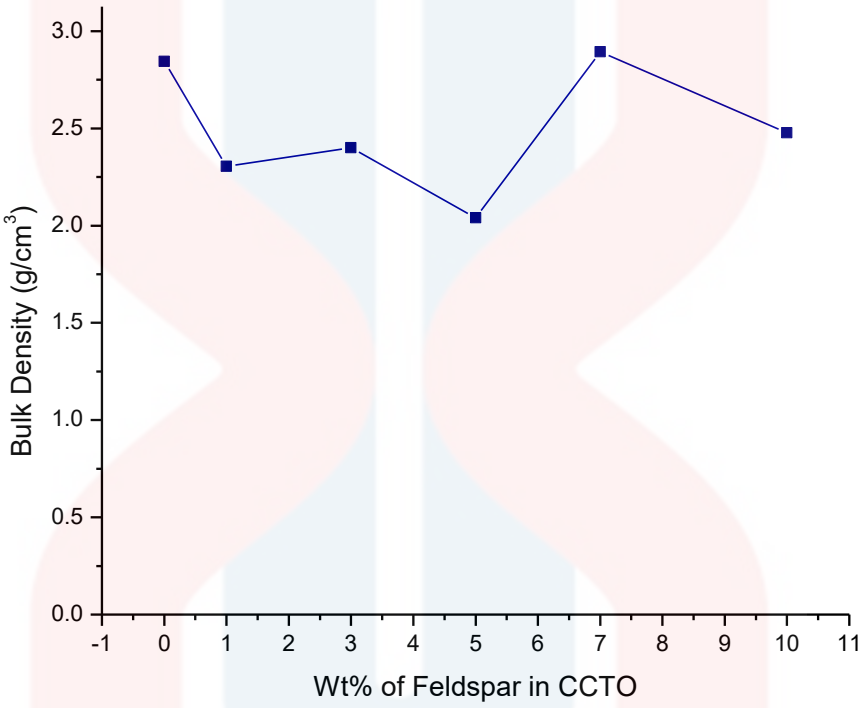

Figure 4.14: Bulk density of as-sintered CCTO

Figure 4.15 show the appearance porosity that formed in the as-sintered CCTO samples. From the graph, the higher density of samples affected the lower porosity.

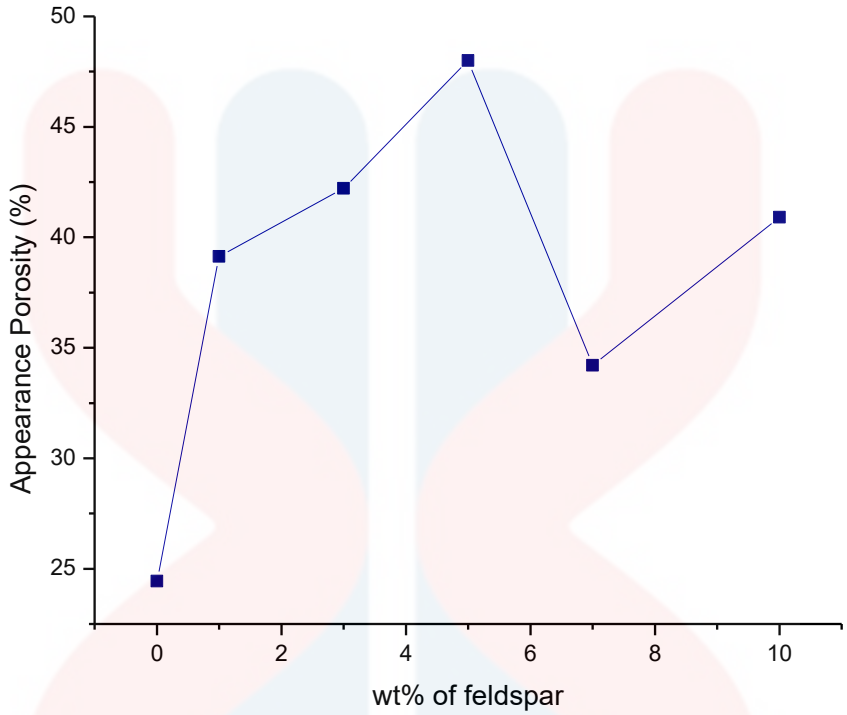

Figure 4.15: Appearance Porosity of sintered CCTO

4.7 Dielectric Constant

Dielectric constant is a number relating the ability of a material to carry alternating current to the ability of vacuum to carry alternating current. The dielectric constant is found to decrease with the increasing of frequency. Figure 4.16 shows the graph of dielectric constant as a function of frequency of weight percentage of feldspar addition in CCTO. The graph shows significant change of dielectric constant as function of frequency happens at frequency range 1-10 MHz. The dielectric constant value is very high at 1 MHz, which is about 4000 for 1% of feldspar addition CCTO. The 10% of feldspar addition CCTO sample give the lowest dielectric constant value compare with other samples which is about 700.

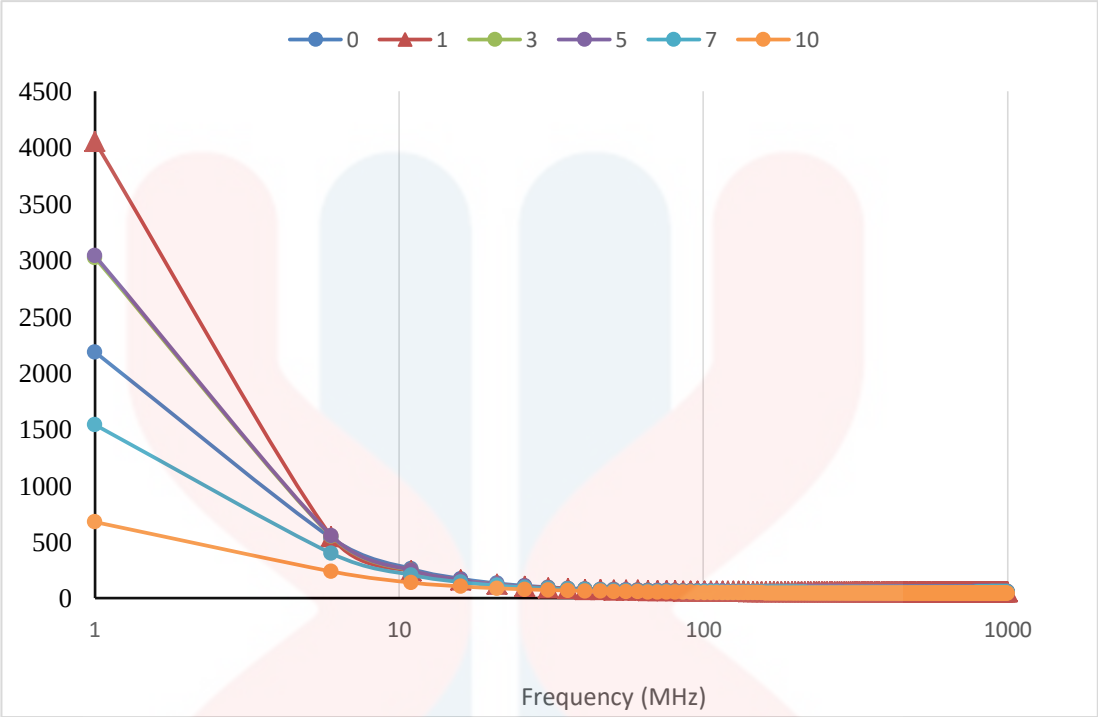

Figure 4.16: Dielectric Constant versus frequency (MHz) of as-sintered CCTO pellets with addition of 0% of feldspar, 1% of feldspar, 3% of feldspar, 5% of feldspar, 7% of feldspar and 10% of feldspar.

4.8 Dielectric Loss

CCTO electroceramic is very suitable used in the resonator, capacitor, memory device and other application because of their high dielectric constant. However, CCTO is not fully applicable because of their dielectric loss is higher. There are many researchers have paid their attention to solve this problem. In this study, feldspar is added to the pure CCTO sample in order to reduce the dielectric loss of this electroceramic. Figure 4.17 shows the frequency dependence of dielectric loss of as-sintered CCTO pellet. At range 0 – 50 MHz, there are peaks of all the CCTO samples. CCTO with 1 wt. % of feldspar have the highest dielectric loss peak compared with 10 wt. % of feldspar added in CCTO with lowest peak.

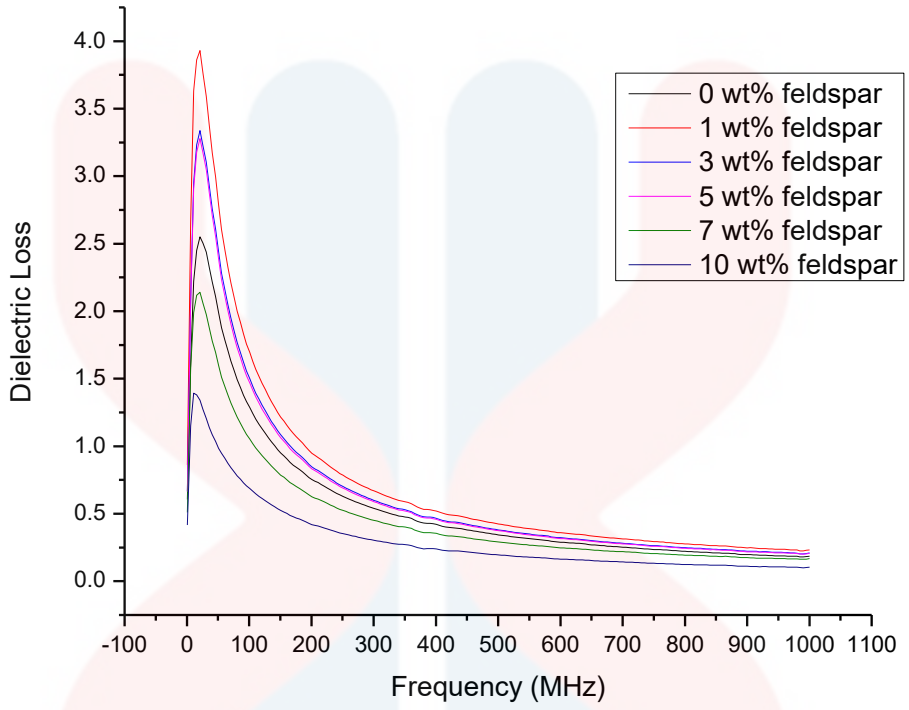

Figure 4.17: Dielectric loss versus frequency (MHz) of as-sintered pellet of CCTO

CHAPTER 5

CONCLUSIONS AND RECOMMENDATIONS

5.1 Conclusion

The objectives of this study are to synthesize pure CCTO and to reduce dielectric loss of CCTO by addition of feldspar. The CCTO phase structure, microstructure and elemental composition also analysed in this study. The effect of dielectric properties was investigated via dielectric constant and dielectric loss analysis. This chapter presented conclusion based on obtained results.

The single phase of CCTO was prepared by using solid state reaction. Processing of samples of CCTO that contains 0, 1, 3, 5, 7 and 10 wt. % of feldspar addition were done at 900°C calcination temperature for 12 hours in furnace. CCTO single phase had completely formed after sintered at 1040°C for 10 hours in furnace. Non-homogeneous mixing process might be contributed to incomplete formation of CCTO during calcination process.

For the surface microstructure analysis using optical microscope (OM), the microstructure of CCTO was found strongly dependent on the weight percentage of feldspar addition. For all as-sintered CCTO, as the weight percentage increases, the average grain size becomes smaller. It is depending on density and porosity of the as-sintered CCTO surface microstructure.

For the dielectric constant analysis, 1% of feldspar addition CCTO shows the highest dielectric constant which is about 4000 while 10% of feldspar addition CCTO shows the lowest dielectric constant which is about 700. For dielectric loss

analysis, as-sintered CCTO with 10 wt. % of feldspar shows the lowest dielectric loss.

5.2 Recommendations

To determine the crystalline size and surface morphology, Field Emission Scanning Electron Microscopy (FESEM) is the suitable equipment that can gives information about grain evolution, grain size, intergranular and intragranular pores of samples. It can reach magnification until 200000X.

The study of CCTO on bulk material had been done by many researchers. CCTO also can be prepared by using chemical reaction method and produce in nanosize for smaller size electronic device application.

REFERENCES

Almeida, A. F. L., De Oliveira, R. S., Góes, J. C., Sasaki, J. M., Souza Filho, A. G., Mendes Filho, J., & Sombra, A. S. B. (2002). Structural properties of CaCu3Ti4O12 obtained by mechanical alloying. *Materials Science and Engineering B: Solid-State Materials for Advanced Technology*, *96*(3), 275–283.

Amaral, F., Costa, L. C., & Valente, M. A. (2011). Decrease in dielectric loss of CaCu3Ti4O12 by the addition of TeO2. *Journal of Non-Crystalline Solids*, *357*(2), 775–781.

Amaral, F., Valente, M., & Costa, L. C. (2010). Synthesis and characterization of calcium copper titanate obtained by ethylenediaminetetraacetic acid gel combustion. *Materials Chemistry and Physics*, *124*(1), 580–586.

Bender, B. a., & Pan, M.-J. (2005). The effect of processing on the giant dielectric properties of CaCu3Ti4O12. *Materials Science and Engineering: B*, *117*(3), 339–347.

Brizé, V., Autret-Lambert, C., Wolfman, J., Gervais, M., Simon, P., & Gervais, F. (2009). Temperature dependence of electron spin resonance in CaCu3Ti4O12 substituted with transition metal elements. *Solid State Sciences*, *11*(4), 875–880.

Brizé, V., Gruener, G., Wolfman, J., Fatyeyeva, K., Tabellout, M., Gervais, M., & Gervais, F. (2006). Grain size effects on the dielectric constant of CaCu 3 Ti 4 O 12 ceramics. *Materials Science and Engineering: B*, *129*(1), 135–138.

Callister, W. D., & Rethwisch, D. G. (2007). *Materials science and engineering: an introduction* (Vol. 7). Wiley New York.

Callister, W., & Rethwisch, D. (2007). *Materials science and engineering: an introduction*. *Materials Science and Engineering* (Vol. 94).

Chen, Y. T., Sheu, C. I., Lin, S. C., & Cheng, S. Y. (2008). Effects of microwave heating on dielectric and piezoelectric properties of PZT ceramic tapes. *Ceramics International*, *34*(3), 621–624.

Felgner, K. H., Müller, T., Langhammer, H. T., & Abicht, H. P. (2004). On the formation of BaTiO3 from BaCO3 and TiO 2 by microwave and conventional heating. *Materials Letters*, *58*(12–13), 1943–1947.

George, S., & Sebastian, M. T. (2009). Three-phase polymer-ceramic-metal composite for embedded capacitor applications. *Composites Science and Technology*, *69*(7–8), 1298–1302.

Huang, X., Jiang, Y., & Wu, K. (2015). CCTO giant dielectric ceramic prepared by reaction sintering. *Procedia Engineering*, *102*, 468–474.

Hutagalung, S. D., Ibrahim, M. I. M., & Ahmad, Z. A. (2008). Microwave assisted sintering of CaCu3Ti4O12. *Ceramics International*, *34*(4), 939–942.

Hutagalung, S. D., Ooi, L. Y., & Ahmad, Z. A. (2009). Improvement in dielectric properties of Zn-doped CaCu3Ti4O12 electroceramics prepared by modified mechanical alloying technique. *Journal of Alloys and Compounds*, *476*(1–2), 477–481.

Jacob, K. T., Rajitha, G., Kale, G. M., Watson, A., & Wang, Z. (2009). High-temperature heat capacity and heat content of CaCu3Ti4O12 (CCTO). *Journal of Alloys and Compounds*, *488*(1), 35–38.

Juliewatty, M. J., Derita, H. S., & Arifin, A. Z. (2009). Influence of sintering parameters on melting CuO phase in CaCu 3Ti4O12. *Malaysian Journal of Microscopy*, *5*(1), 164–170.

Li, T., Chen, Z., Su, Y., Su, L., & Zhang, J. (2009). Effect of grain size and Cu-rich

phase on the electric properties of CaCu3Ti4O12 ceramics. *Journal of Materials Science*, *44*(22), 6149–6154.

Marinescu, I. D. (2007). *Handbook of Advanced Ceramics Machining*. *Ceramics*.

Marques, V. P. B., Ries, A., Simões, A. Z., Ramírez, M. A., Varela, J. A., & Longo, E. (2007). Evolution of CaCu3Ti4O12 varistor properties during heat treatment in vacuum. *Ceramics International*, *33*(7), 1187–1190.

Mei, L. T., Hsiang, H. I., & Fang, T. T. (2008). Effect of copper-rich secondary phase at the grain boundaries on the varistor properties of CaCu3Ti4O12 ceramics. *Journal of the American Ceramic Society*, *91*(11), 3735–3737.

Mohamed, J. J., Hutagalung, S. D., Ain, M. F., Deraman, K., & Ahmad, Z. A. (2007). Microstructure and dielectric properties of CaCu3Ti4O12 ceramic. *Materials Letters*, *61*(8–9), 1835–1838.

Moulson, A. J., & Herbert, J. M. (2003). *Electroceramics: materials, properties, applications*. John Wiley & Sons.

Ni, L., & Chen, X. M. (2009). Enhanced giant dielectric response in Mg-substituted CaCu3Ti4O12 ceramics. *Solid State Communications*, *149*(9–10), 379–383.

Obstler;Mimi. (2012). Ceramic Raw Materials Understanding Ceramic Glaze Materials and Clay Making Ingredients.

Panneerselvam, M., Agrawal, A., & Rao, K. J. (2003). Microwave sintering of MoSi2-SiC composites. *Materials Science and Engineering A*, *356*(1–2), 267–273.

Prakash, B. S., & Varma, K. B. R. (2007). Influence of sintering conditions and doping on the dielectric relaxation originating from the surface layer effects in CaCu3Ti4O12 ceramics. *Journal of Physics and Chemistry of Solids*, *68*(4), 490–502.

Putjuso, T., Manyum, P., Yamwong, T., Thongbai, P., & Maensiri, S. (2011). Effect of annealing on electrical responses of electrode and surface layer in giant-permittivity CuO ceramic. *Solid State Sciences*, *13*(11), 2007–2010.

Rahaman, M. N. (2006). *Ceramic processing*. Wiley Online Library.

Rai, A. K., Mandal, K. D., Kumar, D., & Parkash, O. (2009). Dielectric properties of lanthanum-doped CaCu3Ti4O12 synthesized by semi-wet route. *Journal of Physics and Chemistry of Solids*, *70*(5), 834–839.

Sakamaki, R., Cheng, B., Cai, J., Lin, Y. H., Nan, C. W., & He, J. (2010). Preparation of TiO2-enriched CaCu3Mn0.1Ti3.9O12 ceramics and their dielectric properties. *Journal of the European Ceramic Society*, *30*(1), 95–99.

Shri Prakash, B., & Varma, K. B. R. (2008). Effect of sintering conditions on the microstructural, dielectric, ferroelectric and varistor properties of CaCu3Ti4O12 and La2/3Cu3Ti4O12 ceramics belonging to the high and low dielectric constant members of ACu3M4O12 (A=alkali, alkaline-earth metal, rar. *Physica B: Condensed Matter*, *403*(13–16), 2246–2254.

Smith, A. E., Calvarese, T. G., Sleight, A. W., & Subramanian, M. A. (2009). An anion substitution route to low loss colossal dielectric CaCu3Ti4O12. *Journal of Solid State Chemistry*, *182*(2), 409–411.

Sulaiman, M. A., Hutagalung, S. D., Mohamed, J. J., Ahmad, Z. A., Ain, M. F., & Ismail, B. (2011). High frequency response to the impedance complex properties of Nb-doped CaCu3Ti4O12 electroceramics. *Journal of Alloys and Compounds*, *509*(18), 5701–5707.

Sulaiman, M. A., Hutagalung, S. D., & Zainal, a. (2013). Heat Treatment Effect with the Electrode Constact of CaCu3Ti4O12. *JOURNAL Of NUCLEAR And Related TECHNOLOGIES*, *10*(2), 43–52.

Sun, D.-L., Wu, A.-Y., & Yin, S.-T. (2007). Structure, properties, and impedance spectroscopy of CaCu3Ti4O12 ceramics prepared by Sol-Gel process. *Journal of the American Ceramic Society*, *91*(1), 169–173.

Thomas, P., Dwarakanath, K., Varma, K. B. R., & Kutty, T. R. N. (2008). Nanoparticles of the giant dielectric material, CaCu3Ti4O12 from a precursor route. *Journal of Physics and Chemistry of Solids*, *69*(10), 2594–2604.

Wang, Z. L. (2004). Nanostructures of zinc oxide. *Materials Today*, *7*(6), 26–33.

Ye, Z.-G. (2013). *Handbook of Advanced Dielectric Piezoelectric Ferroelectric Materials:Synthesis, properties and applications*. *Journal of Chemical Information and Modeling* (Vol. 53).

Yun, S., & Wang, X. (2006). Dielectric properties of bismuth doped Ba1-xCaxTiO3 ceramics. *Materials Letters*, *60*(17–18), 2211–2213.

Zhu, B., Wang, Z., Zhang, Y., Yu, Z., Shi, J., & Xiong, R. (2009). Low temperature fabrication of the giant dielectric material CaCu3Ti4O12 by oxalate coprecipitation m ethod. *Materials Chemistry and Physics*, *113*(2–3), 746–748.

APPENDIX A

X-ray data for CCTO raw materials

Pattern: COD 9015691 Radiation: 1.54060 Quality: Quality Unknown

Formula C Ca O3
Name
Name (mineral) Calcite
Name (common)

Lattice: Hexagonal
S.G.: R -3c (167)

a = 4.97710
b =
c = 17.33690
a/b = 1.00000
c/b = 3.48333

alpha =
beta =
gamma =
Z =

Mol. weight =
Volume [CD] = 371.92
Dx =
Dm =
I/Icor = 3.200

- Cuenca, Spain:

Primary Reference
Antao S. M., Hassan I., "Temperature dependence of the structural parameters in the transformation of aragonite to calcite, as determined from in situ synchrotron powder X-ray-diffraction data Note: T = 540 C Note: P = 101 kPa", The Canadian Mineralogist 48 (2010) 1225-1236.

Radiation:
Wavelength: 1.54060
SS/FOM:

Filter: Not specified
d-spacing:

d	2θ	I	h	k	l
3.85950	23.025	80	-1	1	-2
3.05630	29.196	999	-1	1	4
2.88950	30.922	16	0	0	-6
2.48850	36.063	141	-2	1	0
2.28560	39.391	143	-2	1	-3
2.09150	43.222	128	-2	2	2
1.93620	46.887	169	-1	1	-8
1.92970	47.054	55	-2	2	-4
1.88560	48.223	168	-2	1	-6
1.62200	56.707	22	-3	1	-1
1.60850	57.226	9	-1	1	10
1.60110	57.515	76	-3	1	2
1.52810	60.542	20	-2	2	8
1.52500	60.678	40	-3	1	-4
1.52330	60.753	15	-2	1	-9
1.47450	62.989	12	-3	1	5
1.44470	64.443	24	0	0	-12
1.43680	64.840	38	-3	0	0
1.36110	68.935	7	-3	1	-7
1.35090	69.530	16	-2	2	-10
1.30220	72.532	18	-3	1	8
1.28650	73.562	4	-3	0	-6
1.28650	73.562	4	-3	0	6
1.24940	76.127	15	-2	1	-12
1.24430	76.495	7	-4	2	0
1.19020	80.662	3	-1	1	-14
1.18720	80.908	15	-3	1	-10
1.18430	81.148	5	-4	1	-2
1.15240	83.892	21	-4	1	4
1.14280	84.760	13	-4	2	-6
1.13280	85.687	2	-3	1	11
1.07370	91.685	5	-2	2	14
1.05090	94.275	7	-1	1	16
1.04830	94.582	1	-2	1	-15
1.04680	94.760	13	-4	1	-8
1.04570	94.891	11	-4	4	4
1.01880	98.241	6	-3	0	-12
1.01880	98.241	6	-3	0	12

Pattern: COD 9015822 Radiation: 1.54060 Quality: Quality Unknown

Formula Cu O
Name
Name (mineral) Tenorite
Name (common)

Lattice: Monoclinic
S.G.: C 1 2/c 1 (15)

a = 4.67760
b = 3.45930
c = 5.12640
a/b = 1.35218
c/b = 1.48192

alpha =
beta = 98.965
gamma =
Z =

Mol. weight =
Volume [CD] = 81.94
Dx =
Dm =
I/Icor = 4.570

- Synthetic:

Primary Reference
Calos N. J., Forrester J. S., Schaffer G. B., "A crystallographic contribution to the mechanism of a mechanically induced solid state reaction Note: milling time = 10 min", Journal of Solid State Chemistry 122 (1996) 273-280.

Radiation:
Wavelength: 1.54060
SS/FOM:

Filter: Not specified
d-spacing:

d	2θ	I	h	k	l
2.76920	32.302	80	-1	-1	0
2.53190	35.425	323	0	0	-2
2.53120	35.435	963	-1	-1	1
2.33940	38.449	999	-1	-1	-1
2.31020	38.955	247	-2	0	0
1.96210	46.231	21	-1	-1	2
1.85670	49.023	295	-2	0	2
1.78730	51.060	14	-1	-1	-2
1.72970	52.890	105	0	-2	0
1.63680	56.148	3	0	-2	-1
1.58780	58.043	158	-2	0	-2
1.50510	61.567	197	-1	-1	3
1.42820	65.279	190	0	-2	-2
1.40830	66.319	149	-3	-1	1
1.40700	66.388	4	-3	-1	0
1.38490	67.589	111	-1	-1	-3
1.38460	67.605	166	-2	-2	0
1.36850	68.510	1	-2	-2	1
1.31170	71.925	3	-3	-1	2
1.30850	72.128	87	-3	-1	-1
1.30490	72.358	1	-2	-2	-1
1.26590	74.962	59	0	0	-4
1.26560	74.983	61	-2	-2	2
1.19430	80.328	2	-1	-1	4
1.19120	80.580	22	-2	0	4
1.16970	82.378	44	-2	-2	-2
1.16540	82.749	54	-3	-1	3
1.16170	83.070	2	-3	-1	-2
1.15510	83.652	40	-4	0	0
1.11880	87.024	17	-4	0	2
1.11270	87.622	1	-1	-1	-4
1.10120	88.775	62	-1	-3	1
1.08390	90.580	34	-1	-3	-1
1.04380	95.119	14	-2	0	-4
1.02160	97.878	28	0	-2	-4
1.01220	99.108	41	-3	-1	-3

Pattern: COD 7103589 Radiation: 1.54060 Quality: Quality Unknown

Formula D0.09 O2 Ti
Name
Name (mineral)
Name (common)

Lattice: Tetragonal
S.G.: I 41/a m d (141)

a = 3.78580
b =
c = 9.50740
a/b = 1.00000
c/b = 2.51133

alpha =
beta =
gamma =
Z = 4

Mol. weight =
Volume [CD] = 136.26
Dx =
Dm =
I/Icor = 5.440

Primary Reference
Chen Wing K, Borghols Wouter J H, Mulder Fokko M, "Direct observation of space charge induced hydrogen ion insertion in nanoscale anatase TiO2.", Chemical communications (Cambridge, England) 47 (2008) 6342-6344.

Radiation:
Wavelength: 1.54060
SS/FOM:

Filter: Not specified
d-spacing:

d	2θ	I	h	k	l
3.51720	25.302	999	-1	0	-1
2.43010	36.961	63	-1	0	-3
2.37680	37.821	203	0	0	-4
2.33260	38.566	70	-1	-1	-2
1.89290	48.026	283	-2	0	0
1.69920	53.915	179	-1	0	-5
1.66680	55.051	176	-2	-1	-1
1.49330	62.107	30	-2	-1	-3
1.48070	62.695	137	-2	0	-4
1.36360	68.791	60	-1	-1	-6
1.33850	70.269	67	-2	-2	0
1.27840	74.106	5	-1	0	-7
1.26450	75.060	103	-2	-1	-5
1.25100	76.012	28	-3	0	-1
1.18840	80.809	5	0	0	-8
1.17240	82.147	7	-3	0	-3
1.16630	82.671	52	-2	-2	-4
1.16090	83.140	19	-3	-1	-2
1.05940	93.289	7	-2	-1	-7
1.05150	94.205	27	-3	0	-5
1.04370	95.131	30	-3	-2	-1
1.01750	98.410	20	-1	0	-9
1.00650	99.872	12	-2	0	-8

Pattern: COD 9010841 Radiation: 1.54060 Quality: Quality Unknown

Formula Al1.04 Ca0.04 K0.65 Na0.31 O8 Si2.96

Name

Name (mineral) Sanidine

Name (common)

Lattice Monoclinic
S.G.: C 1 2/m 1 (12)

Mol. weight =
Volume [CD] = 706.58
Dx =
Dm =
I/Icor = 0.740

a = 8.43700
b = 13.00300
c = 7.17200
a/b = 0.64885
c/b = 0.55157

alpha =
beta = 116.10 0
gamma =
Z =

Primary Reference
Menna M., Tribaudino M., Renzulli A., "Al-Si order and spinodal decomposition texture of sanidine from igneous clasts of Stromboli (southern Italy): insights into the timing between the emplacement of a shallow basic sheet intrusion and the eruption of related ejecta Locality: Stromboli volcano, southern Italy", European Journal of Mineralogy 20 (2008) 183-190.

Radiation Wavelength : 1.54060
SS/FOM:

Filter: Not specified
d-spacing:

d	2θ	I	h	k	l	d	2θ	I	h	k	l
6.84640	13.515	3	-1	-1	0	2.22430	40.524	13	-2	-2	3
6.50160	13.609	91	0	-2	0	2.21670	40.631	5	-1	-3	-2
6.44070	13.736	60	0	0	-1	2.19570	41.076	106	-1	-5	-1
5.83110	15.182	154	-1	-1	1	2.16210	41.743	4	-3	-3	0
4.57660	19.384	6	0	-2	-1	2.16720	41.640	216	0	-6	0
4.16220	21.330	308	-2	0	1	2.14690	42.053	4	0	0	-3
3.90620	22.735	569	-1	-1	-1	2.14460	42.096	16	-3	-1	3
3.76530	23.464	1	-2	0	0	2.11060	42.811	95	-2	-4	-1
3.76220	23.629	618	-1	-3	0	2.10520	42.926	4	-1	-6	2
3.61020	24.640	168	-1	-3	1	2.08200	43.429	46	-4	0	1
3.60940	24.566	63	-2	-2	1	2.08110	43.449	16	-4	0	2
3.46650	25.754	716	-1	-1	2	2.06940	43.707	31	-1	-3	3
3.27320	27.223	979	-2	-2	0	2.05400	44.052	51	0	-6	-1
3.26190	27.319	366	-2	0	2	2.04660	44.169	9	-2	0	-2
3.25080	27.414	164	0	-4	0	2.03760	44.427	3	-3	-1	-1
3.22030	27.679	999	0	0	-2	1.98200	45.741	126	-4	-2	2
2.97760	29.986	607	-1	-3	-1	1.95410	46.432	111	-2	-2	-2
2.91660	30.640	68	-2	-2	2	1.94370	46.695	37	-3	-3	3
2.90210	30.788	75	0	-4	-1	1.92220	47.249	6	-2	-6	1
2.88570	30.964	118	0	-2	-2	1.91360	47.474	2	-2	-4	3
2.76270	32.380	121	-1	-3	2	1.90610	47.670	14	-3	-5	1
2.74510	32.593	2	-3	-1	1	1.89420	47.991	111	-4	0	0
2.57400	34.827	141	-3	-1	2	1.89220	48.045	38	-4	0	3
2.56200	34.995	166	-2	-4	1	1.88110	48.346	38	-2	-6	0
2.56230	35.132	37	-2	-2	-1	1.86270	48.855	42	-3	-3	-1
2.53330	35.404	160	-1	-1	-2	1.84760	49.275	6	-3	-5	2
2.47920	36.203	175	-3	-1	0	1.84310	49.409	45	-1	-1	-3
2.46700	36.389	11	-2	-4	0	1.83260	49.711	2	-1	-5	-2
2.45970	36.501	1	-1	-5	0	1.81660	50.120	27	-4	-2	0
2.41570	37.169	112	-1	-5	1	1.81660	50.173	6	-4	-2	3
2.36720	37.960	11	-2	0	3	1.81160	50.321	6	-3	-5	0
2.35690	38.163	74	-3	-3	1	1.80510	50.521	46	-2	-5	2
2.31740	38.829	11	-1	-1	3	1.80410	50.551	1	-1	-7	0
2.30260	39.089	18	-2	-4	2	1.79790	50.736	66	0	-6	-2
2.28760	39.352	11	0	-4	-2	1.79260	50.892	252	-2	0	4
2.24590	40.117	18	-3	-3	2	1.79160	50.932	72	0	-4	-3

APPENDIX B

Calculation on starting materials needs to prepare 50 grams of pure CCTO

The chemical reaction is shown as Equation A1. The molecular weight is shown below:

$CaCO_3$ (s) + 3CuO (s) + $4TiO_2$ (s) $\longrightarrow$ $CaCu_3Ti_4O_{12}$ (s) + CO_2 (s)

$CaCO_3$ = 40.078 + 12.011 + 3(15.999) = 100.086 g/mol

3CuO = 3(63.546 + 15.999) = 238.635 g/mol

$4TiO_2$ = 4[47.867 + 2(15.999)] = 319.46 g/mol

Mole of $CaCu_3Ti_4O_{12}$ = mass / relative molecular mass = 50 / [40.078+3(63.546)+4(47.867)+12(15.999)] = 0.0814 g/mol

Based on Equation A1, amount of $CaCO_3$, CuO and TiO_2 needed are:

$CaCO_3$ = 0.0814 x 100.086 = 8.147g

3CuO = 0.0814 x 238.635 = 19.425g

$4TiO_2$ = 0.0814 x 319.46 = 26.004g

APPENDIX C

Calculation on preparation of CCTO with addition of feldspar

The equations to prepare those samples are:
(100 – x wt) CCTO + x wt % Feldspar
Sample weight 50g

When x = 1
99 wt CCTO + 1 wt % feldspar
0.99 x 50g = 49.5g of CCTO
0.01 x 50g = 0.5g of feldspar

When x = 3
97 wt CCTO + 3 wt % feldspar
0.97 x 50g = 48.5g CCTO
0.03 x 50g = 1.5g feldspar

When x = 5
95 wt CCTO + 1 wt % feldspar
0.95 x 50g = 47.5g CCTO
0.05 x 50g = 2.5g feldspar

When x = 7
93 wt CCTO + 7 wt % feldspar
0.93 x 50g = 46.5g CCTO
0.07 x 50g = 3.5g feldspar

When x = 10
90 wt CCTO + 10 wt % feldspar
0.9 x 50g = 45g CCTO
0.1 x 50g = 5.0 g feldspar

APPENDIX D

Bulk density calculation

Bulk density (g/cm^3) = (M_D / M_w - M_s) x density of H_2O (0.997300 ~ 1)

Where,

M_D: mass of sample before vacuum

M_S: mass of sample in water

M_W: mass of sample after vacuum

Sample	M_D (g)	M_S (g)	M_W (g)
X0	0.128	0.094	0.139
X1	0.106	0.078	0.124
X3	0.108	0.082	0.127
X5	0.102	0.076	0.126
X7	0.110	0.085	0.123
X10	0.109	0.083	0.127

For X0

(0.128 / 0.139-0.094) x 1 = 2.8444

For X1

(0.106 / 0.124-0.078) x 1 = 2.3043

For X3

(0.108 / 0.127-0.082) x 1 = 2.4

For X5

(0.102 / 0.126-0.076) x 1 = 2.04

For X7

(0.11 / 0.123-0.085) x 1 = 2.8947

For X10

(0.109 / 0.127-0.083) x 1 = 2.4773

APPENDIX E

Apparent porosity calculation

Apparent porosity (%) = $(M_W - M_D / M_W - M_S) \times 100\%$

For X0

(0.139-0.128 / 0.139-0.194) x 100 = 24.4444%

For X1

(0.124-0.106 / 0.124-0.078) x 100 = 39.1304%

For X3

(0.127-0.108 / 0.127-0.082) x 100 = 42.2222%

For X5

(0.126-0.102 / 0.126-0.076) x 100 = 48%

For X7

(0.123-0.110 / 0.123-0.085) x 100 = 34.2105%

For X10

(0.127-0.109 / 0.127-0.083) x 100 = 40.9091%